

UNIVERSITY OF CAPE TOWN

**PIONS AND VECTOR MESONS AT
FINITE TEMPERATURE
FROM QCD SUM RULES**

By

Mirela Simona Fetea

A THESIS

Submitted to the Faculty of Science
of the University of Cape Town
in partial fulfillment of the requirements for
the degree of Doctor of Philosophy

Department of Physics
February 1998

The University of Cape Town has been given
the right to reproduce this thesis in whole
or in part. Copyright is held by the author.

The copyright of this thesis vests in the author. No quotation from it or information derived from it is to be published without full acknowledgement of the source. The thesis is to be used for private study or non-commercial research purposes only.

Published by the University of Cape Town (UCT) in terms of the non-exclusive license granted to UCT by the author.

DST 530 FE TE

98/17079

Abstract

The temperature corrections to the current algebra Gell-Mann, Oakes and Renner(GMOR) relation in $SU(2) \otimes SU(2)$, the temperature behaviour of the pion mass and the q^2 and T dependence of the $\rho\pi\pi$ vertex function in the space-like region are investigated.

There are no corrections at the leading order in quark masses for GMOR. At the next order, the corrections are of the form $m_q^2 \cdot T^2$, which are small except near critical temperature.

The pion mass is essentially constant, except near critical temperature, where it increases with T .

At the critical temperature $g_{\rho\pi\pi}(q^2, T)$ vanishes independently of q^2 , signalling deconfinement. The extrapolation of the form factor to $q^2 = 0$ is used to show that the pion radius increases with temperature and diverges at temperatures approaching the critical temperature.

In the absence of experimental data at finite temperature, the agreement between the theoretical results obtained using sum rules together with Vector Meson Dominance and using a direct determination, was taken as evidence in support of Vector Meson Dominance at finite temperature.

Contents

1	Introduction	7
1.1	Quantum Chromodynamics	7
1.2	QCD Sum Rules at $T = 0$	8
1.3	QCD Sum Rules at $T \neq 0$	12
2	Introduction to zero temperature QCD	15
2.1	QCD Lagrangian	15
2.2	Regularization (dimensional) and renormalization	19
3	Finite temperature formalism	23
3.1	Finite Temperature Green's functions.	23
3.2	Spinless Bose fields	23
3.3	Fermion fields	26
3.4	Renormalization at finite temperature	28
4	Pions	31
4.1	Gell-Mann Oakes Renner Relation	31
4.2	Gell-Mann Oakes Renner Relation at Finite Temperature	36
4.3	Pion mass	43
5	$\rho\pi\pi$ Coupling	45
5.1	Vector Meson Dominance	45
5.2	$g_{\rho\pi\pi}$ at zero temperature	46
5.3	$g_{\rho\pi\pi}$ at finite temperature	54

<i>CONTENTS</i>	4
5.4 The mean square pion radius	61
6 Conclusion	65
6.1 Conclusion	65
6.2 Critical Assessment of the QCD Sum-Rule Approach	66
Acknowledgements	69
Appendices	70
A Generalities	71
A.1 Notations and conventions	71
A.2 γ -Algebra	72
A.3 Generators for the fundamental representation of $SU_c(3)$	74
B Currents and operators	75
C Dimensional regularization	77
C.1 Feynman's parametrization	77
C.2 Some integrals	78
C.3 Logarithmic integrals	79
C.4 Integrals involving δ -functions	80
C.5 Some useful integrals	83
D Some calculations	85
D.1 Some integral evaluations	85
D.2 A few more detailed steps to determine the final form of $F(s, s', Q^2, T)$	86
Bibliography	87

List of Figures

1.1	Graphical representation of the two-point function $\Pi(q^2)$. The lines are indicating the current, and the blob stands for all possible diagrams which end in a quark-antiquark pair at the vertices.	10
2.1	Graphical representation of the quark propagator $S_{\alpha\beta}^{AB}$	17
2.2	Graphical representation of the quark propagator $D_{ab}^{\mu\nu}$	18
2.3	Graphical representation of the fermionic vertex $S_{\beta\beta'}$	19
2.4	Graphical representation of the triple gluon vertex	20
4.1	Graphical representation of the two-point function $\Pi_{5\mu}$	32
4.2	Showing $f_\pi^2(T)/f_\pi^2(0)$, $s_o(T)/s_o(0)$ and $\langle\bar{q}q\rangle_T / \langle\bar{q}q\rangle_o$ plotted against T/T_c from [2]	39
4.3	Showing RGMOR plotted against T/T_c	41
4.4	Showing the comparison between the chiral perturbation theory and sum rules numerical evaluations of $M_\pi^2 F_\pi^2 / \hat{m} \langle\bar{q}q\rangle$	42
4.5	The ratio $\mu_\pi(T)/\mu_\pi(0)$ obtained by solving the first two sum rules. The solid line corresponds to the first sum rule calculations, the dotted one to the second sum rule.	43
5.1	Graphical representation for the three-point function $\Pi_\mu(q)$	48
5.2	Graphical representation of the lowest order QCD contribution to $g_{\rho\pi\pi}$	48
5.3	Graphical representation of the lowest order QCD contribution to $g_{\rho\pi\pi}$. The explicit momenta appear on each quark line.	50
5.4	Rho-meson dominance diagram with the explicit coupling constants.	50

- 5.5 The integration region in the ss' plane. The solid and dashed lines are the boundaries of the integration region after the subtraction of the continuum in "square" and "triangle" versions. 52
- 5.6 Showing the electromagnetic pion form factor at $T = 0$, determined from the QCD-FESR without invoking VMD- curve (a)-compared with the result of the independent QCD-FESR for $g_{\rho\pi\pi}$ plus VMD- curve (b). Curve (a) represents a fit to the data from Bebek et al., Phys.Rev. D17 (1978) 16. 55
- 5.7 The first order loop diagrams contributing to $\Pi(q, T)$. In the diagrams, a straight internal quark line indicates a zero temperature propagator and a line with a slash through it indicates a quark propagator with the thermal insertion. 56
- 5.8 The ratio of the $\rho\pi\pi$ form factors at finite and zero temperature as functions of T/T_c . Both curves were obtained in chiral limit, but for different values of Q^2 59
- 5.9 The ratio of the $\rho\pi\pi$ form factors at finite and zero temperatures as a function of T/T_c , for $Q^2 = 1 \text{ GeV}^2$. The solid line corresponds to the chiral limit calculations and the dotted line to calculations away from chiral limit. 60
- 5.10 $g_{\rho\pi\pi}/f_\rho$ as a function of Q^2 , plotted for various constant temperatures. 61
- 5.11 The ratio of the (strong) pion radius at finite and at zero temperatures as a function of T/T_c . The solid line corresponds to $Q^2 = 0.3 \text{ GeV}^2$ and the dashed line corresponds to $Q^2 = 0.4 \text{ GeV}^2$ 63

Chapter 1

Introduction

1.1 Quantum Chromodynamics

Most high-energy physicists will readily agree that quantum chromodynamics (QCD) is today the well established theory of strong interactions; at least it has no serious competitor.

Quantum chromodynamics is a non-abelian gauge field theory whose gauge group is the color group $SU(3)$. There are $3^2 - 1 = 8$ gauge bosons that mediate the interactions between the matter particles, called gluons, and the matter particles are spin $\frac{1}{2}$ quarks. Gluons are massless spin 1 bosons, as are the photons, but unlike the photons, they interact among themselves directly because they also carry colour charge. The up and down quarks could be taken in some applications as massless since their mass, of the order of a few MeV , is much smaller than the characteristic energy scale. Quantum chromodynamics is a renormalizable field theory. The coupling constant g is a function of the energy scale Q : $g(Q)$ (running coupling constant) and it tends to zero as the inverse of the logarithm of the energy scale when the energy scale tends to infinity. This is the famous property of asymptotic freedom which allows one to use perturbation theory at high energies, or more precisely in processes with large-momentum transfers, so called "hard processes". When the energy scale decreases, the coupling constant increases, which leads to a breakdown of perturbation theory as a series expansion in powers of $g(Q)$. Thus, "soft processes", processes at small-

momentum transfers, or low energy properties of hadrons (mass spectrum, resonance widths, scattering lengths...) cannot be studied by using perturbation theory. Therefore an alternative expansion scheme or an approach to directly approximate QCD nonperturbatively had to be developed.

The QCD sum-rule approach (introduced by Shifman, Vainshtein and Zakharov in the late 1970's [58] to describe mesonic properties) has proven to be a useful way of extracting both qualitative and quantitative information about hadronic physics (masses and coupling constants) from QCD inputs.

For zero temperature and zero density vacuum, quarks and gluons are confined in hadrons. No free quark or gluon can be observed. The situation may change when the temperature rises above a temperature estimated nowadays to be $\sim 150 \div 200 \text{ MeV}$, called the critical temperature T_c . The system undergoes at this temperature one or maybe two phase transitions with disappearance of the confinement and restoration of chiral symmetry. Then one can obtain a gas of almost free quarks and gluons (quark-gluon plasma-QGP).

The structure of hadrons at finite temperature ($T \neq 0$) receives growing interest in relation to the physics of the hot hadronic matter and QGP.

1.2 QCD Sum Rules at $T = 0$

QCD sum rules formalism approaches the bound state problem in QCD from the asymptotic freedom side. It starts at short distances and moves towards large distances where confinement effects become important, asymptotic freedom starts to break down.

Shifman has compared the strategy of sum-rule approach to the quantum mechanical many-body problem of some external objects injected into a complicated medium. Over time, the external objects interact with themselves and with the medium and will eventually develop into an approximate stationary state with a finite life time. The medium is the QCD vacuum and the external objects are quarks or gluons with definite quantum numbers created by external currents. The approximate stationary

state with a finite life time is the hadronic resonance. The properties of the medium, seen by the quarks, are characterized by vacuum matrix elements of quark and gluon fields called condensates.

In standard perturbation theory these matrix elements vanish after normal ordering.

The nonvanishing vacuum expectation values such as :

$$\langle 0 | \bar{q}q | 0 \rangle \text{ and } \langle 0 | G_{\mu\nu}^a G_{\mu\nu}^a | 0 \rangle$$

signal the breakdown of the asymptotic freedom by the emergence of power corrections due to non perturbative effects in the QCD vacuum. The chiral condensate is often taken as the order parameter for spontaneous chiral symmetry breaking.

QCD sum rules are using momentum space correlation functions (also called correlators) of local composite operators (currents). Each current is constructed using quark or/and gluon fields which carry the quantum numbers (J, P and C) of the hadron which is studied.

A current has the general form:

$$j_{\Gamma}(x) = \bar{q}_i \Gamma q_j$$

where i and j denote the flavor of the quarks and Γ the tensor structure ($\Gamma = 1, \gamma_{\mu}, \gamma_5, \dots$) see Appendix B.

The correlator can be a function of two or more currents.

A two point function is given by:

$$\Pi(q^2) = i \cdot \int dx \cdot e^{iqx} \cdot \langle 0 | T (j_{\Gamma}(x), j_{\Gamma}^{\dagger}(0)) | 0 \rangle \quad (1.1)$$

The two-point function is represented in fig. 1.1, where the vertex Γ depends on the current and the blob represents all the possible diagrams which end in a quark-antiquark pair at the vertices. T denotes the time ordered product and $|0\rangle$ is the physical nonperturbative vacuum state.

The basic idea of QCD sum rules is to match a QCD description of an appropriate correlation function with a phenomenological one. The underlying concept is "duality", which establishes a correspondence between a description in terms of physical

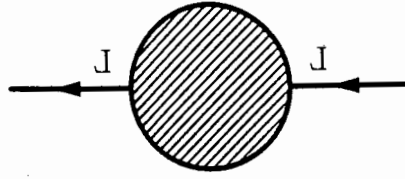


Figure 1.1: Graphical representation of the two-point function $\Pi(q^2)$. The lines are indicating the current, and the blob stands for all possible diagrams which end in a quark-antiquark pair at the vertices.

(hadronic) degrees of freedom and one based on the quark and gluons degrees of freedom.

A QCD sum rule calculation consists of three parts:

- an approximate description of the QCD part of the correlation function via an ‘operator product expansion’ (OPE);
- the description of the same correlator in terms of physical intermediate states via a ‘dispersion relation’;
- a procedure to match the two descriptions and to extract the parameters of interest that characterize the hadronic part;

The OPE [63] expresses a correlator as a sum of products between c-number coefficients and vacuum expectation values of some operators (\hat{O}_n). The c-number coefficients, called Wilson coefficients, obey renormalization group equations and depend on the parameters of the theory, and on the Lorentz indices and quantum numbers of $j_\Gamma(x)$ and \hat{O}_n . The operators \hat{O}_n are local gauge invariant operators constructed from quark and gluon fields. The vacuum expectation values of the composite local gauge-invariant operators are called condensates.

$$\Pi(q^2) = C_I \cdot \langle I \rangle + \sum_n C_n(q) \cdot \langle \hat{O}_n \rangle_{vac} \quad (1.2)$$

The operators \hat{O}_n in equation 1.2 are ordered by increasing dimension, and $C_n(q)$ fall off by corresponding powers of q^2 . At short distances the operators with the lowest dimensions dominate, and give power corrections to the perturbative contributions stemming from the unit operator $\langle I \rangle$. The essence of OPE is the separation of short and long distance physics, the separation between perturbative physics (the coefficients) and nonperturbative physics (the condensates). This suggests that the coefficients can be calculated from QCD via perturbation theory to any desired order in the strong coupling constant [58], while the nonperturbative physics is isolated in vacuum condensates. The sum rules are predictive because a relatively small number of condensates dominate the description of many observables.

The values of the vacuum condensates in the OPE cannot be calculated analytically from first principles. They are extracted from certain channels where experimental information is available (e.g. e^+e^- annihilation, τ decays) or they are estimated numerically from lattice calculations.

At short distances the operators with the lowest dimension dominate. The unit operator in (equation 1.2) has dimension $d = 0$ and $C_I \cdot \langle I \rangle$ stands for the purely perturbative contribution. Since we are interested only in the vacuum expectation values, we only have to consider spin zero operators. The higher dimensional operators are listed in Appendix B.

Expression (1.2) is an expansion in inverse powers of Q^2 and thus is useful in deep spacelike region, for which $Q^2 = -q^2$ is large and positive.

Renormalizable field theories can give good arguments only in perturbation theory about the validity of an expansion like 1.2. Because nonperturbative effects are included, the validity of OPE in the presence of these effects could be questioned. Both the coefficients and the condensates could, in general, contain perturbative as well as nonperturbative contributions. However, in practice, the simplified version described above is used (coefficients are evaluated in perturbation theory while the vacuum expectation values describe the nonperturbative contributions). The use of this simplified version is justified by the phenomenological success of QCD sum rules. There seems to be a “window” in QCD where the simplified version of OPE applies [49].

Different choices of the weight in the dispersion relation lead to different kinds of QCD sum Rules (Hilbert, Laplace or Gaussian transforms, Finite Energy Sum Rules). Each of them has advantages as well as shortcomings. If QCD could be solved exactly and if OPE would be complete (i.e. in absence of nonlocal other contributions) all these sum rules would give the same results.

The exact correlator $\Pi(s)$ ($s = q^2$), is an analytic function in the whole complex plane cut along the positive semi-axis with the branch point at the physical threshold. If $W(s)$ is a holomorphic function in the analytic region of $\Pi(s)$ such that $W(s^*)^* = W(s)$ (the weight function), using the Cauchy theorem one gets:

$$\oint_{C_{s_0}(|s|=s_0)} \Pi(s) \cdot W(s) ds = -2i \cdot \int_{s_{th}}^{s_0} W(s) \cdot \text{Im} \Pi(s) ds \quad (1.3)$$

where C_{s_0} is the circle of radius s_0 . The most popular types of QCD sum rules are: finite-energy sum rules (FESR), where the weight function is $W(s) = s^N$, N being an integer and Laplace sum rule (LSR), where the weight function is $W(s) = \exp(-s/M^2)$. LSR emphasizes the low-energy part of the hadronic spectral function whereas FESR enhances the high-energy region. FESR needs a very accurate parametrization of the spectral function in order to control the propagation of the experimental errors of the data, but has the advantage that it yields a set of decoupled equations for the condensates. The results depend strongly on the asymptotic freedom threshold s_0 . The value of s_0 can be guessed from the data using the first FESR (i.e. $N = 0$). On the other hand, LSR do not require an exact parametrization of the data because the intermediate and high-energy regions and their rather big errors are suppressed. The inconvenience of LSR is that condensates of different dimensions are present and they are strongly correlated [33].

1.3 QCD Sum Rules at $T \neq 0$

At zero temperature the shape of a typical hadronic spectral function consists of some delta functions plus resonances with increasing widths, followed by a smooth continuum starting at some threshold s_0 . From fits to actual data, it is known that

the continuum is well approximated by perturbative QCD. Assuming that the quark deconfinement takes place at some critical temperature T_d , one would expect that by increasing the temperature, the resonance peaks in the spectral function should become broader. At T_d the resonance widths would then become infinite, signalling quark deconfinement. The resonance melting when the temperature is increased, would be accompanied by a shift of the asymptotic freedom threshold s_o . The threshold is expected to depend on the temperature. When the temperature is raised $s_o(T)$ would approach the origin. However, in calculations done in [2] and also from lattice calculations it was remarked that either the deconfinement and chiral-symmetry restoration phase transitions coincide or they occur at extremely similar temperatures

A generalization of QCD sum rules for finite temperature was proposed some time ago [9]. It was assumed that:

- the OPE continues to be valid, but now the vacuum condensates will develop an *a-priori* unknown T -dependence;
- the duality QCD-Hadron remains valid.

In matter with nonzero temperature it is not the causal but the retarded or advanced Green function that posses useful analytical properties [39]. For a two-point function, the basic object to be considered at finite temperature is the retarded (advanced) two point function:

$$\Pi(q^2, T) = i \cdot \int dx \cdot e^{iqx} \cdot \theta(x_o) \cdot \langle\langle [j_R(x), j_R^\dagger(0)] \rangle\rangle \quad (1.4)$$

where $\langle\langle \dots \rangle\rangle$ stands for Gibbs averaging:

$$\langle\langle A \cdot B \rangle\rangle = \sum_n \exp\left(-\frac{E_n}{T}\right) \langle n | A \cdot B | n \rangle / \text{Tr}(\exp(-\frac{H}{T})) \quad (1.5)$$

$|n\rangle$ is a complete set of eigenstates of the QCD-Hamiltonian ($H|n\rangle = E|n\rangle$). The operator product expansion of $\Pi(q^2, T)$ -expression 1.2- can be written now as:

$$\Pi(q^2, T) = C_I \cdot \langle\langle I \rangle\rangle + \sum_m C_m(q) \cdot \langle\langle \hat{O}_m \rangle\rangle \quad (1.6)$$

The states $|n\rangle$ in expression 1.5 can be in principle any complete set of states (e.g. hadronic (mostly pion) states, gluonic states). It was suggested in [27] that at $T < T_c$ the suitable set of states is the set of hadronic states because the original particles forming the heat bath, which is probed by external currents, are hadrons, while the summation over the quark-gluon basis of states would require taking into account the full range of their interaction. The quark-gluon basis was first proposed in [9]. The two approaches are complementary [19], as the information they provide is different. The pion basis is suitable to determine the temperature dependence of vacuum condensates at low T . It does not make use of the QCD-hadron duality and has little relationship to the sum-rules program. The use of the quark-gluon basis (relying on both OPE and QCD-hadron duality) allows a smooth extension of the program to finite T .

Beyond perturbation theory, the validity of the OPE, at any temperature, cannot be proven from first principles since one does not know how to solve QCD exactly. However, at $T = 0$ one can solve exactly other field theories which bear some resemblance to QCD, thus providing evidence in support of the assumption.

It has been suggested [27] that the QCD-hadron duality is not applicable at finite temperature. No singular dynamical mechanism of a discontinuous nature that would invalidate QCD-hadron duality was proposed. At very low temperatures the hadronic spectrum is expected to change very little and the external current will still convert into quark-antiquark pairs. The temperature dependence of the quark and gluon condensates is known and at very low T they also hardly change. It is reasonable to assume that nothing drastic will happen to duality at low temperature. There is a sort of temperature inertia [15] affecting both QCD and hadronic physics at very low T . At finite temperature, though, there are some new effects that must be considered. There are contributions to the QCD and hadronic spectral functions in the space-like region (as opposed to only the time-like region at $T = 0$) and the heat bath can support condensates with non-trivial quantum numbers. However, these contributions vanish smoothly as T approaches zero.

Chapter 2

Introduction to zero temperature

QCD

2.1 QCD Lagrangian

Gell-Mann and Zweig in 1964 postulated that the physical hadrons are composite objects, made up of three quarks (baryons) or a quark-antiquark pair (mesons). The quarks, spin 1/2 particles, are known as the six flavours: u (up), d (down), s (strange), c (charm), b (bottom) and t (top) and carry quantum numbers as isospin, strangeness, etc. Being spin one-half objects, quarks should obey Fermi-Dirac statistics and their states should be antisymmetric. A new internal quantum number was introduced -colour- so that each species of quark may come in any of the three colours $\alpha = r, y, v$ (red, yellow, violet). The physical hadrons are colourless, they are singlets under rotations in colour space.

If $q^i(x)$ denote the quark fields, and if quarks are elementary, as it is usual for spin $\frac{1}{2}$ fields, the Lagrangian density for free quarks can be written as

$$\mathcal{L}_{quarks} \approx \mathcal{L}_o(x) = \sum_{q=u,d,\dots} \sum_j \bar{q}^j(x) (i \not{\partial} - m_q) q^j(x) \quad (2.1)$$

where the metric $g^{\mu\nu} = (1, -1, -1, -1)$ is used.

Renormalizable, unified theories of weak and electromagnetic interactions have shown that, to avoid catastrophic violations of parity to order α , the strong interactions

act on other quantum numbers than flavour. The gluons carry colour, and interact between themselves. Weak and electromagnetic interactions are colour blind. Taking the eight vector gluons, B_a^μ , $a = 1$ to 8 in the adjoint representation of $SU_c(3)$, interacting universally with all quark flavors:

$$\mathcal{L}_1 = \mathcal{L}_o + g \sum_q \sum_{ika} \bar{q}^i(x) \gamma_\mu t_{ik}^a q^k(x) B_a^\mu(x) \quad (2.2)$$

where t^a matrices are $t^a = \frac{1}{2} \lambda^a$, with λ the Gell-Mann matrices (see Appendix A.3). The standard QCD Lagrangian density:

$$\mathcal{L}_{QCD} = \mathcal{L}_1 - \frac{1}{4} \sum_a G_a^{\mu\nu}(x) G_{a\mu\nu}(x) \quad (2.3)$$

$$G_a^{\mu\nu} = \partial^\mu B_a^\nu - \partial^\nu B_a^\mu + g \sum f_{abc} B_b^\mu B_c^\nu$$

Invariance under global transformations has direct physical consequences, like charge conservation. Invariance under local transformations does also have direct physical consequences. The corresponding conserved current, and its associated charge, are gauge dependent, but it does imply extensive relations among Green's functions (Slavnov-Taylor identities). The invariance under local transformations implies a zero gluon mass, fact verified by Rutherford-like angular dependence of high p_t hadronic jets. It is customary to split the Lagrangian density \mathcal{L} into \mathcal{L}_o and \mathcal{L}_{int} where \mathcal{L}_o is obtained from \mathcal{L} setting all interactions equal to zero and $\mathcal{L}_{int} = \mathcal{L} - \mathcal{L}_o$.

In quantum field theory, all interesting physical quantities are derivable from the n -point Green's functions which are defined as the vacuum expectation value of the time-ordered product of n fields:

$$G(x_1, x_2, \dots, x_n) = \langle 0 | T(\xi(x_1)\xi(x_2)\dots\xi(x_n)) | 0 \rangle \quad (2.4)$$

where $\xi(x)$ stands for a generic field. In Heisenberg representation:

$$\xi(t, \vec{x}) = \exp(itH)\xi(0, \vec{x}) \exp(-itH)$$

and $|0\rangle$ is the physical vacuum or ground state of H , which is defined by:

$$H|0\rangle = 0; \langle 0|0\rangle = 1,$$

where H is the full Hamiltonian of the theory in the Heisenberg representation.

The evaluation of the connected Green's functions in the perturbation theory is given by the Gell-Mann-Low relation:

$$G(x_1, x_2, \dots, x_n) = \frac{\langle 0 | T(\xi(x_1)\xi(x_2)\dots\xi(x_n) \exp [i \int d^4x \mathcal{L}_{int}^{(0)}(x)]) | 0 \rangle}{\langle 0 | T(\exp [i \int d^4x \mathcal{L}_{int}^{(0)}(x)]) | 0 \rangle} \quad (2.5)$$

$\mathcal{L}_{int}^{(0)}$ is the interaction Lagrangian density and the upperindex means that all the fields must be taken as free, $|0\rangle$ is the vacuum on which all the annihilation operators appearing in the expansion of the free fields are acting. The denominator in expression 2.5 is precisely the sum of all vacuum to vacuum transition amplitudes and it cancels the disconnected vacuum graphs appearing in the calculation of the numerator.

The two point Green's functions associated with the fields appearing in the theory are the so-called propagators. For example, in momentum space representation:

- the quark propagator (α refers to colour degrees of freedom and A refers to flavour) (see fig.2.1) can be written as:

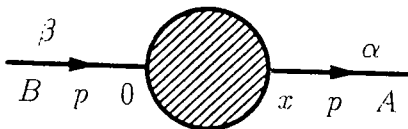


Figure 2.1: Graphical representation of the quark propagator $S_{\alpha\beta}^{AB}$.

$$iS_{\alpha\beta}^{AB}(\not{p}) = \int d^4x \exp(ipx) \langle 0 | T(q_{\alpha}^A(x) \bar{q}_{\beta}^B(0)) | 0 \rangle = i\delta_{\alpha\beta} \delta^{AB} S(\not{p}) \quad (2.6)$$

and - the gluon propagator (see fig.2.2):

can be written as:

$$iD_{ab}^{\mu\nu}(k) = \int d^4x \exp(ikx) \langle 0 | T(B_a^{\mu}(x) B_b^{\nu}(0)) | 0 \rangle = i\delta_{ab} D^{\mu\nu}(k) = i\delta_{ab} D^{\nu\mu}(k) = i\delta_{ab} D^{\mu\nu}(-k) \quad (2.7)$$

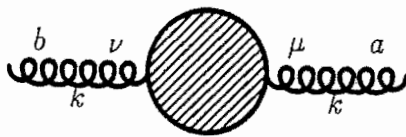


Figure 2.2: Graphical representation of the quark propagator $D_{ab}^{\mu\nu}$.

In the lowest order of perturbation theory they turn out to be:

$$iS_{\alpha\beta}^{(0)AB}(\not{p}) = i\delta_{\alpha\beta}\delta^{AB} \frac{1}{\not{p} - m_A + i\eta} \quad (2.8)$$

and

$$iD_{ab}^{(0)\mu\nu}(k) = i\delta_{ab} \left[-g_{\mu\nu} + (1-a) \frac{k^\mu k^\nu}{k^2 + i\eta} \right] \frac{1}{k^2 + i\eta} \quad (2.9)$$

where a is the gauge fixing constant ($a = -1$ in Fermi-Feynman gauge and $a = 0$ in Landau or transverse gauge).

Three point Green's functions, corresponding to the triple vertex functions appearing in \mathcal{L}_{QCD} (corresponding proper vertex functions which are Green functions with amputated legs) are, for example:

- for the fermionic vertex (see fig.2.3):

$$\begin{aligned} & iS_{\beta\beta'}(-k)ig\Gamma_{\mu'\beta'\alpha'}^a(q, k, p)iS_{\alpha\alpha'}(\not{p})iD_{\alpha'a}^{\mu\mu'}(q) \\ &= \int d^4x d^4y \exp(-ikx) \exp(-ipy) \langle 0 | T(q_\beta(x) \bar{q}_{\alpha'}(y) B_a^\mu(0)) | 0 \rangle \end{aligned} \quad (2.10)$$

with $p + q + k = 0$ (the flavour index was omitted).

and - for the triple gluon vertex (see fig.2.4):

$$\begin{aligned} & igT_{\alpha'b'c'}^{\mu'\nu'\sigma'}(p, q, k)iD_{\mu\mu'}^{a'a}(p)iD_{\nu\nu'}^{b'b'}(q)iD_{\sigma\sigma'}^{c'c}(k) \\ &= \int d^4x d^4y \exp(-ipx) \exp(-iqy) \langle 0 | T(B_\mu^a(x) B_\nu^b(y) B_\sigma^c(0)) | 0 \rangle \end{aligned} \quad (2.11)$$

with $p + q + k = 0$.

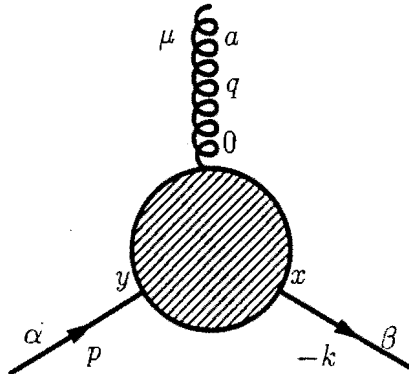


Figure 2.3: Graphical representation of the fermionic vertex $S_{\beta\beta'}$.

2.2 Regularization (dimensional) and renormalization

The lowest-order calculation in quark-gluon processes generally reproduces the parton model results. The Feynman rules allow us to calculate Feynman diagrams at the tree level (without loop diagrams) in the perturbative expansion based on QCD Lagrangian. But the dynamical effect of QCD does not show up at this level. When the rules are applied to calculate diagrams with loops, one finds divergent integrals due to the behaviour of the integrands at high virtual momenta (ultraviolet divergences) and divergences due to the behaviour of the integrands at low virtual momenta (infrared divergences). A meaning must be given to the integrals. Although the divergences are subtracted out in the final physical answer on the basis of the renormalization program, in the intermediate stage, one still requires that the divergent integrals be mathematically manageable. The procedure which makes the integrals finite is called regularization. It amounts to altering the Lagrangian \mathcal{L} to \mathcal{L}_ε in such a way that \mathcal{L}_ε produces finite answers, and in some sense, as $\varepsilon \rightarrow 0$, $\mathcal{L}_\varepsilon \rightarrow \mathcal{L}$.

Any regularization must destroy some physical feature of the theory. If Lattice regularisation, the most powerful regulator for nonperturbative QCD is not used, because

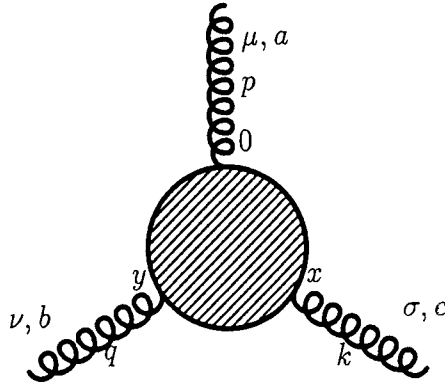


Figure 2.4: Graphical representation of the triple gluon vertex .

gauge and relativistic invariance are essential for QCD, the dimensional regularization is used. It only destroys the scale invariance.

The calculations are done in an arbitrary dimension, $D - \varepsilon$; with the physical limit $\varepsilon \rightarrow 0$.

If a convergent integral is of the form :

$$(2\pi)^D \int d^D k f(k^2); \quad f(k^2) = \frac{(k^2)^r}{(k^2 - a^2)^m}; \quad (2.12)$$

with r and m integers and

$$d^D k = d^0 k d^1 k \dots d^{D-1} k; \quad k^2 = (k^0)^2 - (k^1)^2 - \dots - (k^{D-1})^2,$$

because f is analytic in the k^0 plane, the integration can be rotated from $(-\infty, \infty)$ to $(-i\infty, i\infty)$ (so called Wick rotation). The integration over $(-\infty, \infty)$ is recovered by defining a new variable $k^0 \rightarrow k^D = ik^0$. Thus, an ordinary Euclidean integral in D dimension is obtained:

$$i \int_{-\infty}^{\infty} \frac{dk^1}{2\pi} \dots \int_{-\infty}^{\infty} \frac{dk^D}{2\pi} f(-k_E^2), \quad k_E^2 = (k^1)^2 + (k^2)^2 + \dots + (k^D)^2 \equiv |k_E|^2 \quad (2.13)$$

If $d^D k_E = d^1 k \dots d^D k$, introducing the polar coordinates $d^D k_E = d|k_E| \cdot |k_E|^{D-1} d\Omega_D$ and using the fact that $\int d\Omega_D = 2\pi^{D/2}/\Gamma(D/2)$ one gets:

$$\int \frac{dk^D}{(2\pi)^D} f = \frac{i}{(2\pi)^{D/2}/\Gamma(D/2)} \int_0^{\infty} d|k_E| \cdot |k_E|^{D-1} f(-|k_E|^2) \quad (2.14)$$

The manipulations are valid for D positive integer, but the last formula can be used to define the integral for arbitrary (even complex) D and arbitrary r and m .

The prescription:

$$\int \frac{dk^4}{(2\pi)^4} \rightarrow \int d^D \hat{k} \equiv \int \frac{dk^D \nu_o^{4-D}}{(2\pi)^D}; \quad D = 4 - \varepsilon \quad (2.15)$$

$$\hat{k}^\mu = \frac{\nu_o^{4/D-1}}{2\pi} k^\mu$$

can be used, thereby explicitly introducing the scale-invariance-breaking arbitrary (but fixed) parameter ν_o with dimensions of $[mass]^{-1}$.

Renormalization takes care of the redefinition of the mass and coupling constant, and the readjustment of the normalization of the Green's functions by suitable multiplicative factors which may eliminate possible infinities in the Green's function¹. At each order of perturbation theory, the process of removing divergencies turns out to be a subtraction of divergent pieces in the one-particle irreducible Green's functions. The question is whether the above subtraction process can consistently be performed to all orders with a finite number of multiplicative factors (renormalization constants) and parameters which will be redefined. The theory for which the above procedure operates is said to be renormalizable. Quantum chromodynamics is a renormalizable field theory.

One should note that the renormalisations are not all multiplicative. Additive renormalisations can also occur.

¹The renormalization is not necessarily directed to the elimination of divergencies. It may be a finite renormalization.

Chapter 3

Finite temperature formalism

3.1 Finite Temperature Green's functions.

The thermodynamic state of the system is defined by the parameter β , the inverse temperature measured in energy units $\beta = \frac{1}{k_B T}$, where k_B is Boltzmann's constant. β can be thought of as a Lagrange multiplier which determines the mean energy of the system. For $\beta \rightarrow \infty$ the zero temperature calculations are regained.

The first step in the finite temperature calculations is the knowledge of the thermal behaviour of quark and gluon propagators. A formalism was developed by Dolan and Jackiw [14] to derive the finite temperature spinless Bose and Fermion propagators. The Green's function in finite temperature field theory is defined by:

$$G_\beta(x_1, x_2, \dots, x_n) = \frac{\text{Tr} \{ \exp(-\beta H) T(\xi(x_1)\xi(x_2)\dots\xi(x_n)) \}}{\text{Tr} \{ \exp(-\beta H) \}} \quad (3.1)$$

where H is the Hamiltonian governing the dynamics of the field $\xi(x)$.

3.2 Spinless Bose fields

The finite-temperature 2-point function of spin-less fields, using expression 3.1, is defined by:

$$D_\beta(x - y) = \frac{\text{Tr} \{ \exp(-\beta H) T(\varphi(x)\varphi(y)) \}}{\text{Tr} \{ \exp(-\beta H) \}} = \langle T(\varphi(x)\varphi(y)) \rangle \quad (3.2)$$

which for non-interacting fields satisfies:

$$(\square_x + m^2) D_\beta(x - y) = -\delta^4(x - y) \quad (3.3)$$

Boundary conditions must be specified in order to solve the above equation. These are given for imaginary time. The time ordering is defined on the complex time interval $[0, -i\beta]$:

$$\langle T(\varphi(x)\varphi(y)) \rangle = \begin{cases} (\varphi(x)\varphi(y)) = D_\beta^>(x - y) & ix_o > iy_o \\ (\varphi(y)\varphi(x)) = D_\beta^<(x - y) & ix_o < iy_o \end{cases} \quad (3.4)$$

and therefore:

$$\begin{aligned} D_\beta(x - y)|_{x_o=0} &= D_\beta^<(x - y)|_{x_o=0} \\ D_\beta(x - y)|_{x_o=-i\beta} &= D_\beta^>(x - y)|_{x_o=-i\beta} \end{aligned} \quad (3.5)$$

which leads to the following periodic boundary conditions:

$$D_\beta(x - y)|_{x_o=0} = D_\beta(x - y)|_{x_o=-i\beta} \quad (3.6)$$

Using expression 3.6, $D_\beta(p)$ can be express as a Fourier transform of $D_\beta(x)$:

$$D_\beta(p) = \int_0^{-i\beta} dx_o \int d^3x \exp(ipx) D_\beta(x) \quad (3.7)$$

where $p^\mu = (\omega_n, \vec{p})$ with $\omega_n = \frac{2\pi n}{-i\beta}$; $n = 0, \pm 1, \dots$

p^μ is a space-like vector because

$$p^2 = \omega_n^2 - \vec{p}^2 = -\left(\frac{4\pi^2 n^2}{\beta^2} + \vec{p}^2\right) \leq 0$$

The imaginary time representation for the Green's function is obtained by substituting equation 3.7 in equation 3.3 and solving for $D_\beta(p)$:

$$D_\beta(p) = \frac{i}{p^2 - m^2} \quad (3.8)$$

By using Fourier integrals, the real time representation of $D_\beta(x - y)$ can be obtained.

By definition, the Fourier transform of $D_\beta^>(x)$ is $\bar{D}_\beta^>(k)$, with:

$$\bar{D}_\beta^>(k) = \int d^4x \exp(ikx) D_\beta^>(x)$$

Then,

$$\begin{aligned}\overline{D}_\beta^<(k) &= \int d^4x \exp(ik_o x_o - \vec{k} \cdot \vec{x}) D_\beta^<(x) = \int d^4x \exp(ik_o x_o - \vec{k} \cdot \vec{x}) D_\beta^>(x_o - i\beta, \vec{x}) \\ &= \exp(-\beta k_o) \int d^4x \exp(ik_o x_o - \vec{k} \cdot \vec{x}) D_\beta^>(x_o, \vec{x}) = \exp(-\beta k_o) \overline{D}_\beta^>(k).\end{aligned}\tag{3.9}$$

Defining the spectral function as:

$$\rho(k) = \overline{D}_\beta^>(k) - \overline{D}_\beta^<(k),$$

equation 3.9 can be written as:

$$\overline{D}_\beta^>(k) = (1 + f(k_o))\rho(k); \quad \overline{D}_\beta^<(k) = f(k_o)\rho(k)\tag{3.10}$$

with:

$$f(k_o) = (\exp(\beta k_o) - 1)^{-1}\tag{3.11}$$

being the thermal Bose-Einstein distribution.

Knowing $\rho(k)$, one can determine $\overline{D}_\beta(k)$, the Fourier integral transform of $D_\beta(x)$:

$$\begin{aligned}\overline{D}_\beta(k) &= \int d^4x \exp(ikx) [\theta(x_o) D_\beta^>(x) + \theta(-x_o) D_\beta^<(x)] \\ &= i \int_{-\infty}^{\infty} \frac{dk'_o}{2\pi} \left[\frac{\overline{D}_\beta^>(k'_o, \vec{k})}{k_o - k'_o + i\varepsilon} - \frac{\overline{D}_\beta^<(k'_o, \vec{k})}{k_o - k'_o - i\varepsilon} \right]\end{aligned}$$

Using the integral form of the θ -functions and substituting equation 3.10 in the above expression, one obtains:

$$\overline{D}_\beta(k) = i \int_{-\infty}^{\infty} \frac{dk'_o}{2\pi} \frac{\rho(k'_o, \vec{k})}{k_o - k'_o + i\varepsilon} + f(k_o)\rho(k)\tag{3.12}$$

The spectral function $\rho(k)$, can be obtained from the imaginary-time representation for $D_\beta(x)$:

$$\begin{aligned}
D_\beta(\omega_n, \vec{k}) &= \int_0^{-i\beta} dx_o \exp(-(2\pi n/\beta)x_o) \int d^3x \exp(-i \vec{k} \cdot \vec{x}) D_\beta(x) \\
&= \int_0^{-i\beta} dx_o \exp(-(2\pi n/\beta)x_o) \int d^3x \exp(-i \vec{k} \cdot \vec{x}) D_\beta^>(x) \\
&= \int_0^{-i\beta} dx_o \exp(-(2\pi n/\beta)x_o) \int_{-\infty}^{\infty} \frac{dk_o}{2\pi} \exp(-ik_o x_o) D_\beta^>(k) \\
&= i \int_{-\infty}^{\infty} \frac{dk_o}{2\pi} \frac{\exp(-i\beta k_o) - 1}{k_o - 2\pi n/(-i\beta)} [1 + f(k_o)] \rho(k) = i \int_{-\infty}^{\infty} \frac{dk_o}{2\pi} \frac{\rho(k_o, \vec{k})}{\omega_n - k_o}
\end{aligned}$$

To determine $\rho(k)$, $D_\beta(\omega_n, \vec{k})$ is extended to a continuous function $D_\beta(k_o, \vec{k})$ and in the limit $\varepsilon \rightarrow 0$:

$$\rho(k) = D_\beta(k_o + i\varepsilon, \vec{k}) - D_\beta(k_o - i\varepsilon, \vec{k})$$

For the free-field case expression 3.8, with $\varepsilon(k_o)$ the sign function, $\rho(k)$ becomes:

$$\rho(k) = 2\pi\varepsilon(k_o)\delta(k^2 - m^2)$$

Substituting $\rho(k)$ in expression 3.12, the real-time Green's function for spinless-Bose fields is:

$$\overline{D}_\beta(k) = \frac{i}{k^2 - m^2 + i\varepsilon} + \frac{2\pi}{\exp(\beta|k_o|) - 1} \delta(k^2 - m^2) \quad (3.13)$$

where $\frac{1}{\exp(\beta|k_o|) - 1} = n_B(|k_o|)$.

3.3 Fermion fields

The Fermion fields formalism is developed analogously to the spinless-Bose fields one.

The anticommutativity of the Fermion fields must be taken into account.

The finite-temperature 2-point function of fermion fields, using equation 3.1, is defined by:

$$S_\beta(x - y) = \frac{\text{Tr} \{ \exp(-\beta H) T(\psi(x)\psi(y)) \}}{\text{Tr} \{ \exp(-\beta H) \}} = \langle T(\psi(x)\psi(y)) \rangle \quad (3.14)$$

which for non-interacting fields satisfies:

$$(i \not{\partial}_x - m) S(x - y) = i\delta^4(x - y) \quad (3.15)$$

Boundary conditions must be specified in order to solve the above equation. These are given for imaginary time. The time ordering is defined on the complex time interval $[0, -i\beta]$:

$$\langle T(\psi(x)\psi(y)) \rangle = \begin{cases} (\psi(x)\psi(y)) = S_\beta^>(x - y) & ix_o > iy_o \\ -(\psi(y)\psi(x)) = S_\beta^<(x - y) & ix_o < iy_o \end{cases} \quad (3.16)$$

and therefore:

$$\begin{aligned} S_\beta(x - y)|_{x_o=0} &= S_\beta^<(x - y)|_{x_o=0} \\ S_\beta(x - y)|_{x_o=-i\beta} &= S_\beta^>(x - y)|_{x_o=-i\beta} \end{aligned} \quad (3.17)$$

These lead to the anti-periodic boundary conditions:

$$S_\beta(x - y)|_{x_o=0} = -S_\beta(x - y)|_{x_o=-i\beta} \quad (3.18)$$

and than, to:

$$S_\beta(p) = \frac{i}{\not{p} - m} \quad (3.19)$$

where $p^\mu = (\omega_n, \vec{p})$ with $\omega_n = \frac{(2n+1)\pi}{-i\beta}$; $n = 0, \pm 1, \dots$

By using Fourier integrals, the real time representation of $S_\beta(x - y)$ can be obtained.

By definition, the Fourier transform of $S_\beta^<(x)$ is $\overline{S}_\beta^<(k)$, with:

$$\overline{S}_\beta^<(k) = \int d^4x \exp(ikx) S_\beta^<(x)$$

Then, analogously to the spinless-Bose case:

$$\overline{S}_\beta^<(k) = \exp(-\beta k_o) \overline{S}_\beta^>(k) \quad (3.20)$$

Defining the spectral function as:

$$\rho(k) = \overline{S}_\beta^>(k) + \overline{S}_\beta^<(k)$$

expression 3.20 can be written as:

$$\overline{S}_\beta^>(k) = (1 - f(k_o))\rho(k); \quad \overline{S}_\beta^<(k) = f(k_o)\rho(k) \quad (3.21)$$

with:

$$f(k_o) = (\exp(\beta k_o) + 1)^{-1} \quad (3.22)$$

being the thermal Fermi-Dirac distribution.

As before, the spectral function $\rho(k)$ can be obtained from the imaginary-time propagator :

$$S(\omega_n, \vec{k}) = \int_0^{-i\beta} dx_o \exp(-(2n+1)\pi/\beta)x_o \int d^3x \exp(-i\vec{k}\vec{x}) S_\beta^>(x) = i \int_{-\infty}^{\infty} \frac{dk_o}{2\pi} \frac{\rho(k_o, \vec{k})}{\omega_n - k_o}$$

To determine $\rho(k)$, $S_\beta(\omega_n, \vec{k})$ is extended to a continuous function $S_\beta(k_o, \vec{k})$ and in the limit $\varepsilon \rightarrow 0$:

$$\rho(k) = S_\beta(k_o + i\varepsilon, \vec{k}) - S_\beta(k_o - i\varepsilon, \vec{k})$$

In the non interacting field case (equation 3.19), $\rho(k)$ becomes:

$$\rho(k) = 2\pi\varepsilon(k_o)(\not{k} + m)\delta(k^2 - m^2).$$

The real-time Green's function for Fermi fields is then:

$$\overline{S}_\beta(k) = \frac{i}{(\not{k} - m) + i\varepsilon} - \frac{2\pi(\not{k} + m)}{\exp(\beta|k_o|) + 1} \delta(k^2 - m^2) \quad (3.23)$$

where $\frac{1}{\exp(\beta|k_o|) + 1} = n_F(|k_o|)$ is the Fermi thermal factor.

There are two important aspects that must be noted in expressions 3.13 and 3.23. First, both of them allow one to separate a zero-temperature part and a thermal part, which vanishes in the $T = 0$ limit. Second, one has to note that is the absolute value $|k_o|$ which is featured in equations 3.13 and 3.23, while k_o appears in equations 3.11 and 3.22.

3.4 Renormalization at finite temperature

In computing loop diagrams at finite temperature, one encounters divergencies which must be taken care of. Fortunately, the renormalization at zero temperature suffices to

make the theory finite at non-zero temperature. The temperature does not modify the theory at short distances $\ll 1/T$ and thus the ultraviolet (short distance) singularities are the same as for $T = 0$.

The real-time expression for the free propagator equation 3.13, for example, can be split into a $T = 0$ part and a T -dependent part:

$$\overline{D}_\beta = \overline{D}_\beta^{T=0} + \overline{D}_\beta^{T \neq 0}$$

the temperature-dependent part containing a factor decreasing at least as:

$$\exp(-\beta |k_0|) \delta(k^2 - m^2) \tag{3.24}$$

Divergencies can only arise from loop integrations $\int d^4k$ which do not contain $\overline{D}_\beta^{T \neq 0}$. The δ -function in equation 3.24 puts the k -line on the shell, and the $\int d^3k$ integration is then damped exponentially. Divergencies could come from integrations over other loop momenta, which do not contain $\overline{D}_\beta^{T \neq 0}$ factors but the corresponding divergencies are taken care of by $T = 0$ counter-terms [6].

It is worth remarking that the formalism presented in this chapter only works at one loop order, but a generalisation with auxiliary fields to higher orders exists.

Chapter 4

Pions

The properties of hadronic matter should change as the temperature or density are increased. A dilute system could be described in terms of pions, nucleons and other hadrons. The spontaneous breaking of chiral symmetry is believed to be a property of the strong interaction at zero temperature. If the temperature is finite, different regimes appear, and for high temperatures the chiral symmetry has to be restored according to asymptotic freedom.

Due to its small mass, the pion plays a special role in the dynamics of hot hadronic matter. When the system is heated, the first particles to be produced are the pions. The low temperature hadronic phase regime is dominated by the lightest particle occurring in the spectrum: the pion.

4.1 Gell-Mann Oakes Renner Relation

The low energy properties of the pions are essentially fixed by chiral symmetry. This leads to a wealth of low-energy theorems derived in current algebra at $T = 0$. For instance, the Gell-Mann Oakes Renner (GMOR) relation relates the pion decay constant and mass to the quark condensate and the quark masses [31]. For two light-quark flavours:

$$f_\pi^2 \cdot \mu_\pi^2 = -(m_u + m_d) \langle \bar{q}q \rangle \quad (4.1)$$

where the decay constant $f_\pi \simeq 93 \text{ MeV}$, $\langle \bar{u}u \rangle \simeq \langle \bar{d}d \rangle \equiv \langle \bar{q}q \rangle \simeq -0.01 \text{ GeV}^3$.

To analyze the temperature corrections to GMOR using sum-rules programme; one should start by studying the zero temperature GMOR.

One could start by considering the following two-point function (at $T = 0$):

$$\Pi_{5\mu} = i \int d^4x \exp(iqx) \langle 0 | T(A_\mu(x) j_5^\dagger(0)) | 0 \rangle \quad (4.2)$$

where $A_\mu(x) =: \bar{d}(x) \gamma_5 \gamma_\mu u(x) :$ and $j_5(x) =: \bar{d}(x) i \gamma_5 u(x) :$. The lowest order Feynman diagram corresponding to expression 4.2, is depicted in fig.4.1.

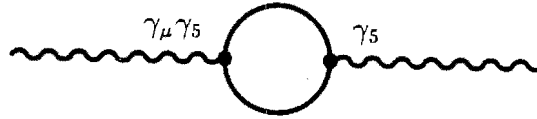


Figure 4.1: Graphical representation of the two-point function $\Pi_{5\mu}$.

One can define:

$$\Pi_{5\mu} = q_\mu \Pi_5 \implies \Pi_5 = \frac{1}{q^2} (q^\mu \Pi_{5\mu}).$$

Using equation 2.6, $\Pi_5(q^2)$ becomes:

$$\Pi_5(q^2) = -\frac{1}{q^2} N_c \int d^4x \exp(iqx) \text{Tr} \left\{ \not{q} \gamma_5 S_F^{(u)}(x) \gamma_5 S_F^{(d)}(-x) \right\}, \quad (4.3)$$

where $N_c = 3$ represents the number of colours. Using 3.19 and working, for example, in momentum space in perturbative QCD for the corrections $\sim m_q$:

$$\begin{aligned} \Pi_5(q^2) = & -\frac{3}{q^2} \int d^4x \exp(iqx) \int \frac{d^4k_1}{(2\pi)^4} \int \frac{d^4k_2}{(2\pi)^4} \exp(-ik_1x) \exp(ik_2x) \\ & \cdot \text{Tr} \left\{ \not{q} \gamma_5 \frac{(\not{k}_1 + m_u)}{k_1^2 - m_u^2} \gamma_5 \frac{(\not{k}_2 + m_d)}{k_2^2 - m_d^2} \right\} \end{aligned} \quad (4.4)$$

with $q - k_1 + k_2 = 0$. By using γ -Algebra, Appendix A.2, $\Pi_5(q^2)$ becomes:

$$\Pi_5(q^2) = -\frac{3}{q^2} \left\{ 4(m_u - m_d) q_\alpha \int \frac{d^4k}{(2\pi)^4} \frac{k^\alpha}{k^2(k-q)^2} - 4m_u q^2 \int \frac{d^4k}{(2\pi)^4} \frac{1}{k^2(k-q)^2} \right\} \quad (4.5)$$

The integrals in expression 4.5 are solved in Appendix C and the term of $\Pi_5(q^2) \sim m_q$, in perturbative QCD, becomes:

$$\Pi_5(q^2) = -i \frac{3}{8\pi^2} (m_u + m_d) \ln\left(-\frac{q^2}{v^2}\right) \quad (4.6)$$

To get the imaginary part ($\text{Im } f(z) = -\frac{1}{2\pi} \text{Disc}f(z)$), Cutkosky's rule $\frac{1}{k^2} \rightarrow -2\pi i \delta(k^2)$ and Appendix C.4 were used.

$$\text{Im } \Pi_5(q^2) = \frac{3}{8\pi} (m_u + m_d) \quad (4.7)$$

For the (nonperturbative) corrections to $\Pi_5(q^2) \sim m_q^2$ one has to look at the quark condensate:

$$\begin{aligned} & \langle 0 | T(A_\mu(x) j_5^\dagger(0)) | 0 \rangle = \\ & = \left\{ (\gamma_\mu \gamma_5)_{ik} (\gamma_5)_{lm} i \left[d_m^b(0) \bar{d}_i^a(x) \langle \bar{u}_l^b(0) u_k^a(x) \rangle + \langle \bar{d}_i^a(x) d_m^b(0) \rangle u_k^a(x) \bar{u}_l^b(0) \right] \right\} \\ & = \frac{\langle \bar{q}q \rangle}{\pi^2} \left(\frac{1}{x^2} + \frac{(m_u + m_d)^2}{16} \right) \frac{x_\mu}{x^2} \end{aligned}$$

Therefore the contribution $\sim m_q^2$ is:

$$\Pi_5(q^2) = \frac{2i \langle \bar{q}q \rangle}{q^2} \left(1 + \frac{(m_u + m_d)^2}{4q^2} \right) \quad (4.8)$$

Another term of $\Pi_5(q^2) \sim m_q$ is the one $\sim \langle \frac{\alpha_s}{\pi} G^2 \rangle$. Defining:

$$\Psi_5(q^2) = i \int d^4x \exp(iqx) \langle 0 | T(\partial^\mu A_\mu(x) \partial^\nu A_\nu^\dagger(0)) | 0 \rangle$$

with

$$\partial^\mu A_\mu(x) = (m_u + m_d) : \bar{d}(x) i \gamma_5 u(x) := (m_u + m_d) j_5(x)$$

then

$$\begin{aligned} q^\mu \Pi_{5\mu} &= q^2 \Pi_5 = i q^\mu \int d^4x \exp(iqx) \langle 0 | T(A_\mu(x) j_5^\dagger(0)) | 0 \rangle \\ &= i \int d^4x \left(\frac{\partial^\mu}{i} \exp(iqx) \right) \langle 0 | T(A_\mu(x) j_5^\dagger(0)) | 0 \rangle = \frac{i}{(m_u + m_d)} \Psi_5 \end{aligned}$$

or

$$\Psi_5(q^2) = -i(m_u + m_d) q^2 \Pi_5(q^2) .$$

We find for Ψ_5 :

$$\Psi_5^{PT} = -\frac{3}{8\pi^2}(m_u + m_d)^2 q^2 \ln\left(-\frac{q^2}{\nu^2}\right)$$

$$\Psi_5^{\langle\bar{q}q\rangle} = 2(m_u + m_d) \langle\bar{q}q\rangle + (m_u + m_d)^3 \frac{\langle\bar{q}q\rangle}{2q^2}$$

which coincide with the known results [5]. From [5] ,

$$\Psi_5^{\langle\frac{\alpha_s}{\pi}G^2\rangle} = -(m_u + m_d)^2 \frac{1}{8q^2} \left\langle \frac{\alpha_s}{\pi} G^2 \right\rangle$$

so that an other term of $\Pi_5(q^2) \sim m_q$ is:

$$\Pi_5^{\langle\frac{\alpha_s}{\pi}G^2\rangle}(q^2) = -i(m_u + m_d) \frac{1}{8q^4} \left\langle \frac{\alpha_s}{\pi} G^2 \right\rangle \quad (4.9)$$

To get the (perturbative) corrections to $\Pi_5(q^2) \sim m_q^3$, the propagators are substituted in equation 4.3. Working in coordinate space:

$$\text{Tr} \left\{ \not{x} \gamma_5 S_F^{(u)}(x) \gamma_5 S_F^{(d)}(-x) \right\} =$$

$$= \text{Tr} \left\{ \not{x} \gamma_5 \left(\frac{\hat{x}}{2\pi^2 x^4} + \frac{im_u}{4\pi^2 x^2} + \frac{m_u^2 \hat{x}}{8\pi^2 x^2} \right) \gamma_5 \left(\frac{\hat{x}}{2\pi^2 x^4} - \frac{im_d}{4\pi^2 x^2} - \frac{m_d^2 \hat{x}}{8\pi^2 x^2} \right) \right\}; \hat{x} = \gamma^\mu x_\mu$$

so that the m_q^3 term is:

$$\frac{-i}{8\pi^4} m_u m_d (m_u + m_d) \frac{q^\alpha x_\alpha}{x^4}.$$

Hence:

$$\Pi_5(q^2) = \frac{3i}{4\pi^2} m_u m_d (m_u + m_d) \frac{1}{q^2} \quad (4.10)$$

The complete expression of $\Pi_5(q^2)$ to order $\mathcal{O}(m_q^3)$ in perturbative QCD with the leading non-perturbative corrections is:

$$\Pi_5(q^2)|_{QCD} = -i \frac{3}{8\pi^2} (m_u + m_d) \ln\left(-\frac{q^2}{\nu^2}\right) - i(m_u + m_d) \frac{1}{8q^4} \left\langle \frac{\alpha_s}{\pi} G^2 \right\rangle$$

$$+ \frac{2i \langle\bar{q}q\rangle}{q^2} + (m_u + m_d)^2 \frac{i \langle\bar{q}q\rangle}{2q^4} + \frac{3i}{4\pi^2} m_u m_d (m_u + m_d) \frac{1}{q^2} \quad (4.11)$$

To get an idea of the importance of various terms at a scale of $q^2 \simeq -1\text{GeV}^2$, we used: $m_u \simeq 5\text{MeV}$; $m_d \simeq 10\text{MeV}$ [20], and $\left\langle \frac{\alpha_s}{\pi} G^2 \right\rangle \simeq (1-4) \times 10^{-2} \text{GeV}^4$ [8]. Hence $\Pi_5(q^2)|_{QCD}$ can be approximated as being:

$$\Pi_5(q^2)|_{QCD} \simeq -i \frac{3}{8\pi^2} (m_u + m_d) \ln\left(-\frac{q^2}{\nu^2}\right) - i(m_u + m_d) \frac{1}{8q^4} \left\langle \frac{\alpha_s}{\pi} G^2 \right\rangle$$

$$+ \frac{2i \langle\bar{q}q\rangle}{q^2} + i(m_u + m_d)^2 \frac{\langle\bar{q}q\rangle}{2q^4} \quad (4.12)$$

By saturating equation 4.2 with the lowest hadronic state, the pion¹, $\Pi_{5\mu}$ becomes:

$$\Pi_{5\mu} = i \int d^4x \exp(iqx) \int_p \langle 0 | A_\mu(x) | \pi(p) \rangle \langle \pi(p) | j_5^\dagger(0) | 0 \rangle$$

Invoking PCAC (partial conservation of the axial vector current) (see [52]),

$$\langle 0 | A_\mu(0) | \pi(p) \rangle = +i\sqrt{2}f_\pi p_\mu$$

$$\langle 0 | \partial^\mu A_\mu | \pi \rangle = (m_u + m_d) \langle 0 | j_5 | \pi \rangle = \sqrt{2}f_\pi \mu_\pi^2$$

with $f_\pi = 93 \text{ MeV}$ (neutral pion) and μ_π the pion's mass. These lead to:

$$\Pi_{5|HAD} = i \frac{2f_\pi^2 \mu_\pi^2}{(m_u + m_d) \mu_\pi^2 - q^2} \quad (4.13)$$

Invoking analyticity, the two point function $\Pi_{5\mu}$, satisfies a dispersion relation :

$$\Pi_{5\mu}(Q^2) = \frac{1}{\pi} \int_0^\infty ds \frac{\text{Im} \Pi_{5\mu}(s)}{s + Q^2}; \quad Q^2 = -q^2$$

defined to a certain number of subtractions which can be disposed of by taking a sufficient number of derivatives.

The QCD-Hadron duality is implemented via expression 1.3. The first two sum rules ($N = 0$ and $N = 1$) in this case are:

$$2f_\pi^2 \mu_\pi^2 = -2(m_u + m_d) \langle \bar{q}q \rangle + \frac{3}{8\pi^2} (m_u + m_d)^2 \int_0^{s_0} ds \quad (4.14)$$

and

$$2f_\pi^2 \mu_\pi^4 = \frac{1}{8} (m_u + m_d)^2 \left\langle \frac{\alpha_s}{\pi} G^2 \right\rangle + \frac{3}{8\pi^2} (m_u + m_d)^2 \int_0^{s_0} s ds \quad (4.15)$$

Equation 4.14 becomes the GMOR relation at leading order in quark masses.²

¹The contributions from higher resonances $:\pi', \pi'' \dots$ are ignored because the analysis is restricted to energies below 1GeV , case in which these hadronic contributions are absorbed in the continuum.

²The explicit form of the trivial integrals appear only to compare them later with the integrals appearing when the temperature corrections are considered.

4.2 Gell-Mann Oakes Renner Relation at Finite Temperature

At finite temperature, the propagators develop a temperature correction (see 3.23), a term containing a Fermi factor. The decay constant f_π , the pion mass μ_π , the continuum threshold s_o , the quark condensate $\langle \bar{q}q \rangle$ and the gluon condensate (basically independent of T except near the critical temperature), $\langle \frac{\alpha_s}{\pi} G^2 \rangle$, become functions of T . To derive *GMOR* relation at finite temperature, one should follow the same steps as in the zero temperature case, the operators are just replaced with their thermal averages.

Π_5 in this case is:

$$\Pi_5(q^2, T) = -\frac{3}{q^2} \int d^4x \exp(iqx) \text{Tr} \left\{ \not{q} \gamma_5 S_F^{(u)T}(x) \gamma_5 S_F^{(d)T}(-x) \right\} \quad (4.16)$$

Using equation 3.23 and working, for example, in momentum space in perturbative QCD for the corrections $\sim m_q$:

$$\begin{aligned} \Pi_5(q^2, T) = & -\frac{3}{q^2} \int d^4x \exp(iqx) \int \frac{d^4k_1}{(2\pi)^4} \int \frac{d^4k_2}{(2\pi)^4} \exp(-ik_1x) \exp(ik_2x) \\ & \cdot \left\{ \text{Tr} \left\{ \not{q} \gamma_5 \frac{(k_1 + m_u)}{k_1^2 - m_u^2} \gamma_5 \frac{(k_2 + m_d)}{k_2^2 - m_d^2} \right\} + \right. \\ & 2\pi i \text{Tr} \left\{ \not{q} \gamma_5 (k_1 + m_u) n_F(|k_{1o}|) \delta(k_1^2 - m_u^2) \gamma_5 \frac{(k_2 + m_d)}{k_2^2 - m_d^2} \right\} + \\ & \left. 2\pi i \text{Tr} \left\{ \not{q} \gamma_5 \frac{(k_1 + m_u)}{k_1^2 - m_u^2} \gamma_5 (k_2 + m_d) n_F(|k_{2o}|) \delta(k_2^2 - m_d^2) \right\} \right\} \end{aligned} \quad (4.17)$$

with $q - k_1 + k_2 = 0$. The fourth trace term (the one with two Fermi factors) does not appear because it is real. One can observe that the first term in expression 4.17 is the one obtained in $T = 0$ case.

By using γ -Algebra (Appendix A.2), $\Pi_5(q^2)$ becomes:

$$\begin{aligned} \Pi_5(q^2, T) = & -\frac{12}{q^2} \left\{ (m_u - m_d) q_\alpha \int \frac{d^4 k}{(2\pi)^4} \frac{k^\alpha}{k^2(k-q)^2} - m_u q^2 \int \frac{d^4 k}{(2\pi)^4} \frac{1}{k^2(k-q)^2} \right\} \\ & + 2\pi i n_F(|k_o|) \delta(k^2 - m_u^2) \int \frac{d^4 k}{(2\pi)^4} \frac{m_u q \cdot (k-q) - m_d q \cdot k}{(k-q)^2 - m_d^2} \\ & + 2\pi i n_F(|(k-q)_o|) \delta((k-q)^2 - m_d^2) \int \frac{d^4 k}{(2\pi)^4} \frac{m_u q \cdot (k-q) - m_d q \cdot k}{k^2 - m_u^2} \end{aligned} \quad (4.18)$$

To get the imaginary part, one could again use Cutkosky's rule $\frac{1}{k^2} \rightarrow -2\pi i \delta(k^2)$. The imaginary part of the first term is the same as for $T = 0$:

$$\frac{3}{8\pi} (m_u + m_d)$$

For the other two terms:

$$\begin{aligned} \text{Im } \Pi_5(q^2, T) = & \frac{24\pi^2}{q^2} \int \frac{d^4 k}{(2\pi)^4} \left((m_u - m_d) q \cdot k - m_u q^2 \right) \\ & \cdot \{ n_F(|k_o|) \delta(k^2 - m_u^2) \delta^+((k-q)^2 - m_d^2) \\ & + m_u q^2 n_F(|(k-q)_o|) \delta((k-q)^2 - m_d^2) \delta^+(k^2 - m_u^2) \} \end{aligned} \quad (4.19)$$

Unlike the zero temperature case (when only annihilation processes appear), at finite temperature there are two distinct processes. One in which the virtual 'quanta' associated with the current will convert into $\bar{q}q$ pairs in the time-like region $q^2 = \omega^2 - \vec{q}^2 \geq 4m_q^2$ (annihilation) and the other for quanta with space-like momenta $q^2 = \omega^2 - \vec{q}^2 \leq 0$ (scattering) will be scattering with quarks in the gas. In the finite temperature case, $\Pi_5(q^2, T)$ has two components: $\Pi_5^{(+)}(q^2, T)$ (annihilation part) and $\Pi_5^{(-)}(q^2, T)$ (scattering part).

Using the results from Appendix C.4 (C.23),

$$\text{Im } \Pi_5^{(+)}(q^2, T) = \frac{3}{8\pi} (m_u + m_d) \left\{ 1 - \frac{1}{2} \int_{-1}^1 dx \left[n_F \left(\frac{|\vec{q}| |x + \omega|}{2} \right) + n_F \left(\frac{|\vec{q}| |x - \omega|}{2} \right) \right] \right\} \quad (4.20)$$

which for a reference frame in which $|\vec{q}| \rightarrow 0$ becomes:

$$\text{Im } \Pi_5^{(+)}(q^2, T) = \frac{3}{8\pi} (m_u + m_d) \left\{ 1 - 2n_F \left(\frac{\omega}{2} \right) \right\} \quad (4.21)$$

and using equation C.24:

$$\text{Im } \Pi_5^{(-)}(q^2, T) = \frac{\pi}{2} T^2 (m_u + m_d) \delta(\omega^2) \quad (4.22)$$

A remark here should be added: by choosing the frame $|\vec{q}| \rightarrow 0$, Lorentz invariance is lost. It is known that finite temperature theories do not preserve Lorentz invariance but the results are not sensitive to the choice of frame.

The temperature corrections have the opposite sign of $T = 0$ part.

From expressions 4.21 and 4.22 one see that for $T \rightarrow 0$ we regain the results at nonzero temperature.

By analogy with the zero temperature case, the first two sum rules ($N = 0$ and $N = 1$), in the finite temperature case are:

$$2f_\pi^2(T)\mu_\pi^2(T) + 2(m_u + m_d) \langle \bar{q}q \rangle_T = \frac{3}{8\pi^2} (m_u + m_d)^2 \left\{ \frac{4\pi^2}{3} T^2 + \int_0^{s_o(T)} ds \left[1 - 2n_F\left(\frac{\sqrt{s}}{2T}\right) \right] \right\} \quad (4.23)$$

and

$$2f_\pi^2(T)\mu_\pi^4(T) = \frac{3}{8\pi^2} (m_u + m_d)^2 \left\{ \frac{\pi}{3} \langle \alpha_s G^2 \rangle_T + \int_0^{s_o(T)} ds s \left[1 - 2n_F\left(\frac{\sqrt{s}}{2T}\right) \right] \right\} \quad (4.24)$$

Where $\omega^2 = s$. The lower limit of the integrals is actually $(m_u + m_d)^2$. However, the difference is of $\mathcal{O}(m_q^4)$. Equation 4.23 becomes the GMOR relation at finite temperature at leading order in quark masses.

The following notations are used:

$$GMOR(0) = 2f_\pi^2\mu_\pi^2 + 2(m_u + m_d) \langle \bar{q}q \rangle \quad (4.25)$$

$$GMOR(T) = 2f_\pi^2(T)\mu_\pi^2(T) + 2(m_u + m_d) \langle \bar{q}q \rangle_T \quad (4.26)$$

and

$$RGMOR = \frac{GMOR(T)}{GMOR(0)} \quad (4.27)$$

The results from [3], away from the chiral limit (i.e. $m_q \neq 0$) were used for the temperature behavior of $\langle \bar{q}q \rangle_T$. The gluon condensate is basically independent of T , except very close to the critical temperature [32]. The temperature behaviour of the

asymptotic freedom threshold s_o , can be obtained from the lowest dimension FESR associated with the two-point function involving the axial-vector currents [21] and [2] provided $f_\pi(T)$ is known [3].

This sum-rule reads:

$$8\pi^2 f_\pi^2(T) = \frac{1}{2} \int_0^{s_o(T)} dz^2 v(z) [3 - v^2(z)] \left[1 - 2n_F\left(\frac{z}{2T}\right) \right] + \int_0^\infty dz^2 v(z) [3 - v^2(z)] n_F\left(\frac{z}{2T}\right)$$

$$\text{where } v(z) = \left(1 - \frac{(m_u + m_d)^2}{z^2} \right)^{\frac{1}{2}}$$

$s_o(T)/s_o(0)$ and $\langle \bar{q}q \rangle_T / \langle \bar{q}q \rangle_0$, as well as the input $f_\pi^2(T)/f_\pi^2(0)$ are shown in fig.4.2

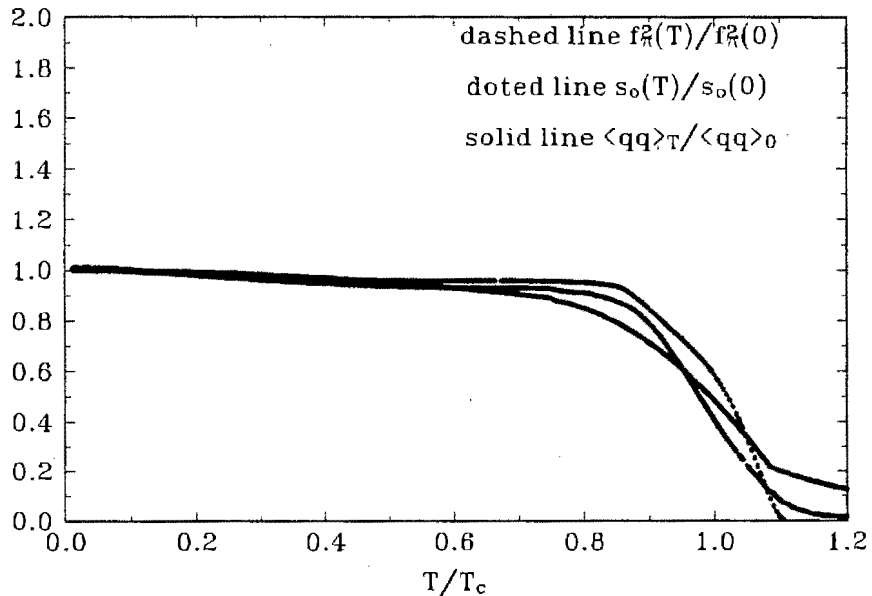


Figure 4.2: Showing $f_\pi^2(T)/f_\pi^2(0)$, $s_o(T)/s_o(T)$ and $\langle \bar{q}q \rangle_T / \langle \bar{q}q \rangle_0$ plotted against T/T_c from [2]

For a wide range of temperatures, not close to T_c , say $T < 0.8T_c$, the following scaling

relation holds with a good approximation:

$$\frac{f_\pi^2(T)}{f_\pi^2(0)} \simeq \frac{\langle \bar{q}q \rangle_T}{\langle \bar{q}q \rangle} \simeq \frac{s_o(T)}{s_o(0)} \quad (4.28)$$

The temperature at which $s_o(T)$ vanishes is the critical temperature for deconfinement (T_d). The temperature at which $f_\pi(T)$ vanishes is the critical temperature for chiral-symmetry restoration (T_c). However, in [2] it was remarked that either the deconfinement and chiral-symmetry restoration phase transitions coincide or they occur at extremely similar temperatures.

Using expressions 4.25 and 4.26, equation 4.27 becomes :

$$RGMOR = \frac{4\pi^2}{3} \frac{T^2}{s_o(0)} + \frac{1}{s_o(0)} \int_0^{s_o(T)} ds \left[1 - 2n_F\left(\frac{\sqrt{s}}{2T}\right) \right] \quad (4.29)$$

The expression 4.29, is not exactly analytically solvable, but it can be computed numerically. The integration was done using a numerical 20 point Gaussian integration routine (positions and weights for the Gaussian integral are from [1]). For $s_o(0) = 1\text{GeV}^2$ (reasonable changes around this value have basically no change in the result) a plot of $RGMOR$ against T/T_c can be seen in fig. 4.3:

The result is in agreement with expectations: since both $f_\pi(T)$ and $\langle \bar{q}q \rangle_T$ decrease with T , the same should be true for $RGMOR$. From sum-rule point of view, the decrease of $RGMOR$ with temperature is due to the decrease of $s_o(T)$ with temperature because in expression 4.29, $T^2/s_o(0) \ll 1$ in the temperature range under consideration.

The result obtained in [61] using chiral perturbation theory expansion, indicate a small deviation linear in pion mass that appears in³:

$$\frac{M_\pi^2 F_\pi^2}{\hat{m} \langle \bar{q}q \rangle} \quad (4.30)$$

when $\mathcal{O}(T^2)$ ⁴ (two-loop, $\mathcal{O}(p^6)$ calculation of the parameters entering $GMOR(T)$) corrections are considered. From dimensional arguments, a linear deviation can not appear in the sum-rules approach. However, the two results agree from numerical point of view. A numerical comparison between the two results is given in fig. 4.4.

³The notation used in [61] is used in 4.30.

⁴The square of pion speed becoming negative define a natural limitation of the $\mathcal{O}(T^2)$ chiral perturbation theory expansion.(see [61])

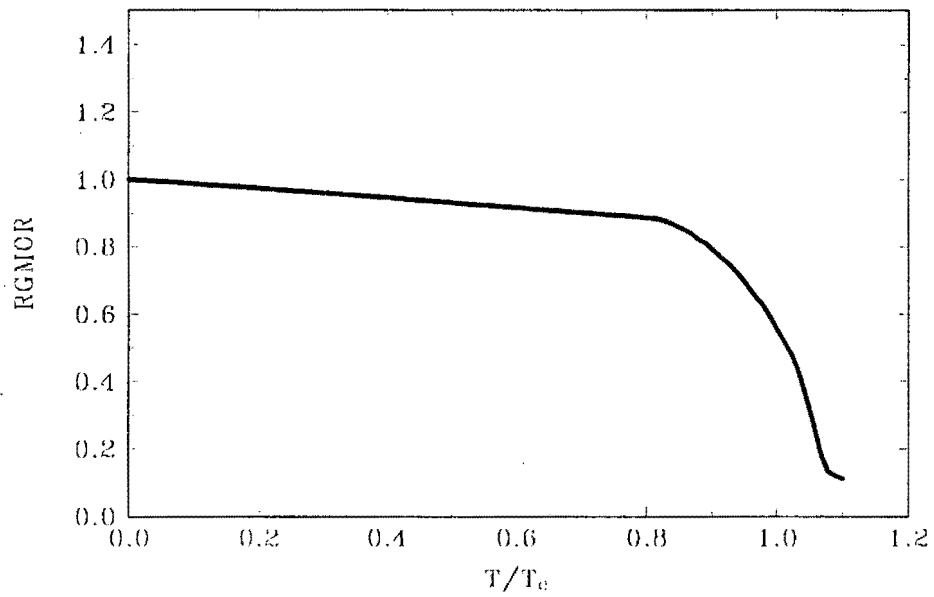


Figure 4.3: Showing RGMOR plotted against T/T_c

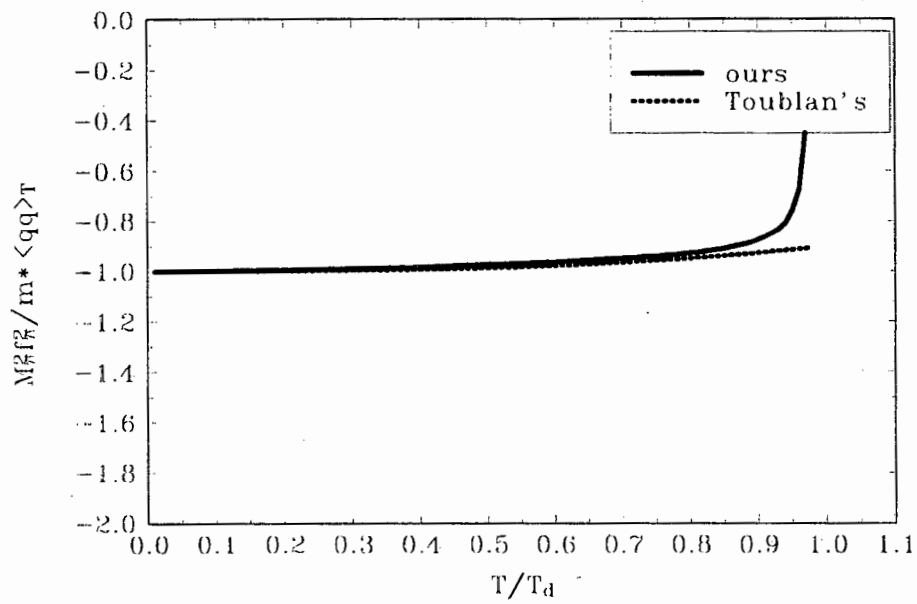


Figure 4.4: Showing the comparison between the chiral perturbation theory and sum rules numerical evaluations of $M_\pi^2 F_\pi^2 / \hat{m} \langle \bar{q}q \rangle$

4.3 Pion mass

The first two sum rules ($N = 0$ and $N = 1$) at zero temperature (equations 4.14 and 4.15) and at finite temperature (equations 4.23 and 4.15) can be used to determine the temperature dependence of the pion mass. For $s_p(0) = 1\text{GeV}^2$ (reasonable changes around this value have basically no change in the result), $C_4 \langle O_4 \rangle \simeq \frac{\pi}{3} \langle \alpha_s G^2 \rangle \simeq 0.07\text{GeV}^4$ ($\langle \alpha_s G^2 \rangle_T = \langle \alpha_s G^2 \rangle - \frac{4\pi^2}{1215} \frac{T^8}{f_\pi^4} (\ln \frac{\Lambda_p}{T} - \frac{1}{4})$ with $\Lambda_p = 275 \pm 65\text{MeV}$ (see [32])) a plot of the ratio of pion mass at finite temperature - pion mass at zero temperature against T/T_c from both sum rules give reasonable results in 20% agreement one with the other (see fig. 4.5).

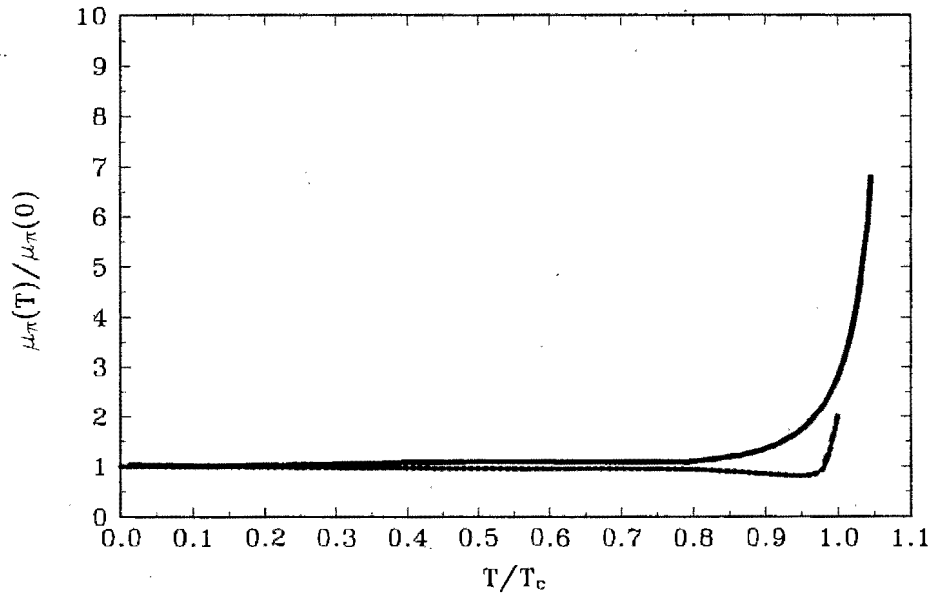


Figure 4.5: The ratio $\mu_\pi(T)/\mu_\pi(0)$ obtained by solving the first two sum rules. The solid line corresponds to the first sum rule calculations, the dotted one to the second sum rule.

On plotting both graphs, 4.28 was used as input.

The pion mass is essentially a constant up to the critical temperature. This result is in agreement with results obtained using other methods (see [30], [40], [57]).

Chapter 5

$\rho\pi\pi$ Coupling

5.1 Vector Meson Dominance

The storage-ring experiments have shown that in the $e^+e^- \rightarrow \pi^+\pi^-$ and $e^+e^- \rightarrow K^+K^-$ processes, the cross sections are dominated by diagrams in which the timelike virtual photon first converts into a vector meson, and then the vector meson decays into the meson-antimeson pair. There was no evidence of a direct decay of the timelike virtual photon into $\pi^+\pi^-$ or K^+K^- pairs. It was reasonable to surmise that the vector mesons contribute significantly to other electromagnetic processes in the spacelike region as well [11].

The Vector Meson Dominance Model (VMD) was created on this assumption. In it, the (spacelike or timelike) virtual photon is interacting with the hadrons only through the known vector mesons (ω and ϕ , the low-mass isoscalar vector mesons, and ρ and ρ' the observed isovector mesons). The vector meson-photon coupling is taken to be almost independent of q^2 . In the model, the pion form factor in the spacelike ($q^2 < 0$) region and in the timelike ($q^2 > 0$) have the same functional dependence. In the spacelike region, the form factor extracted from data on the electroproduction of pions [34], indicates that in this region the pion form factor is dominated by the ρ meson.

The temperature variation of the electromagnetic pion form factor, is an important information, required to calculate the dilepton production rates, in hadronic phase.

It was usually assumed in these calculations that VDM remains valid at non zero temperature, and, with few exceptions [22], that the ρ meson mass and width are temperature independent. The validity of VMD at finite temperature is checked in the next sections, by using the coupling constant $g_{\rho\pi\pi}(Q^2)$ determined from the sum rules (assuming the validity of VMD) and comparing the resulting pion form factor with the data. At finite temperature, it is compared with a theoretical result not relying on VDM.

5.2 $g_{\rho\pi\pi}$ at zero temperature

The two point functions programme, used to determine masses and decay widths, was followed by its extension to the problem next in complexity, namely the determination of dynamic characteristics of resonances such as their electromagnetic form factors and three-hadron vertices based only on the fundamental properties of QCD. The extension for a certain quark current consists in the replacement of the two-point functions with the three-point functions and the replacement of the dispersion relation by a double dispersion relation.

Consider the three-point function:

$$\Pi_\mu(q) = i^2 \cdot \iint d^4x d^4y \exp(-iq \cdot y) \cdot \exp(ip' \cdot x) \times \langle 0 | T(j_\pi^\dagger(x) J_\mu^\rho(y) j_\pi(0)) | 0 \rangle \quad (5.1)$$

where $J_\mu^\rho(y)$ $j_\pi(x)$ are the usual ρ and π currents:

$$J_\mu^\rho(y) = \frac{1}{2} : [\bar{u}(y) \gamma_\mu u(y) - \bar{d}(y) \gamma_\mu d(y)] : \quad (5.2)$$

$$j_\pi(x) = (m_u + m_d) : \bar{d}(x) i\gamma_5 u(x) : \quad (5.3)$$

$\Pi_\mu(q)$ can be written as:

$$\Pi_\mu(q) = \Pi_1(q^2)P_\mu + \Pi_2(q^2)q_\mu \quad (5.4)$$

with $P_\mu = (p' + p)_\mu$ and $q_\mu = (p' - p)_\mu$

In the euclidean region $p^2, p'^2, q^2 < 0$, where the virtualities are large enough, $\Pi_\mu(q)$

can be calculated in the framework of perturbative QCD. The corresponding graphs are depicted in fig. 5.2.

By analogy with steps taken in the two-point function case,

$$\begin{aligned} \Pi_\mu(q) = & \frac{i}{2} N_c (m_u + m_d)^2 \text{Tr} \left\{ \iint d^4x d^4y \exp(-iq \cdot y) \cdot \exp(ip' \cdot x) \int \frac{d^4k_1}{(2\pi)^4} \int \frac{d^4k_2}{(2\pi)^4} \int \frac{d^4k_3}{(2\pi)^4} \right. \\ & [\exp(-ik_1 \cdot x) \exp(ik_2 \cdot y) \cdot \exp(-ik_3(y-x)) \cdot \gamma_5 \cdot S(k_1) \cdot \gamma_5 \cdot S(k_2) \cdot \gamma_\mu \cdot S(k_3) - \\ & \left. \exp(ik_1 \cdot x) \exp(-ik_2 \cdot y) \cdot \exp(-ik_3(x-y)) \cdot \gamma_5 \cdot S(k_3) \cdot \gamma_\mu \cdot S(k_2) \cdot \gamma_5 \cdot S(k_1)] \right\} \end{aligned} \quad (5.5)$$

with $N_c = 3$ (the number of colours) and k_1 , k_2 and k_3 depicted in fig.5.3.

The first term in expression 5.5 comes from diagram (a) and the second term from diagram (b). In the first diagram: $k_2 = k_1 - p$ and $k_3 = k_1 - p'$ and in diagram (b) : $k_2 = k_1 + p$ and $k_3 = k_1 + p'$ so that:

$$\begin{aligned} \Pi_\mu(q) = & \frac{i}{2} N_c (m_u + m_d)^2 \int \frac{d^4k}{(2\pi)^4} \cdot \\ & \left\{ \text{Tr} (\gamma_5 \gamma_\alpha \gamma_5 \gamma_\beta \gamma_\mu \gamma_\gamma) \cdot \frac{k_\alpha (k-p)_\beta (k-p')_\gamma}{k^2 (k-p)^2 (k-p')^2} - \text{Tr} (\gamma_5 \gamma_\alpha \gamma_\mu \gamma_\beta \gamma_5 \gamma_\gamma) \cdot \frac{k_\gamma (k+p)_\beta (k+p')_\alpha}{k^2 (k+p)^2 (k+p')^2} \right\} \end{aligned} \quad (5.6)$$

but

$$\frac{k_\gamma (k+p)_\beta (k+p')_\alpha}{k^2 (k+p)^2 (k+p')^2} \xrightarrow{k \rightarrow -k} - \frac{k_\gamma (k-p)_\beta (k-p')_\alpha}{k^2 (k-p)^2 (k-p')^2}$$

Using γ -Algebra from Appendix A.2, $\Pi_\mu(q)$ becomes:

$$\begin{aligned} \Pi_\mu(q) = & -4i \cdot N_c (m_u + m_d)^2 \int \frac{d^4k}{(2\pi)^4} \cdot \frac{1}{k^2 (k-p)^2 (k-p')^2} \cdot \\ & \left\{ (k-p')_\mu k \cdot (k-p) + (k-p)_\mu k \cdot (k-p') - k_\mu (k-p)(k-p') \right\} \end{aligned} \quad (5.7)$$

After a few calculations, to leading order in α_s and quark masses (see Appendix D.1):

$$\Pi_\mu(q) = \frac{3}{8\pi^2} \cdot (m_u + m_d)^2 (p+p')_\mu \ln\left(-\frac{q^2}{\nu^2}\right) \quad (5.8)$$

The next step is to calculate the imaginary part of $\Pi_\mu(q)$. The contact with the "hadronic" world is done by using the double dispersion relation:

$$\Pi(p^2, p'^2) = \frac{1}{\pi^2} \int ds \int ds' \frac{\text{Im} \Pi(s, s')}{(s-p^2)(s'-p'^2)} \quad (5.9)$$

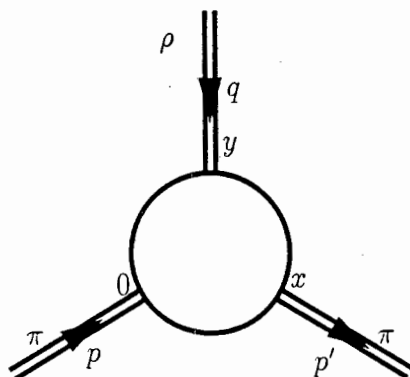


Figure 5.1: Graphical representation for the three-point function $\Pi_\mu(q)$.

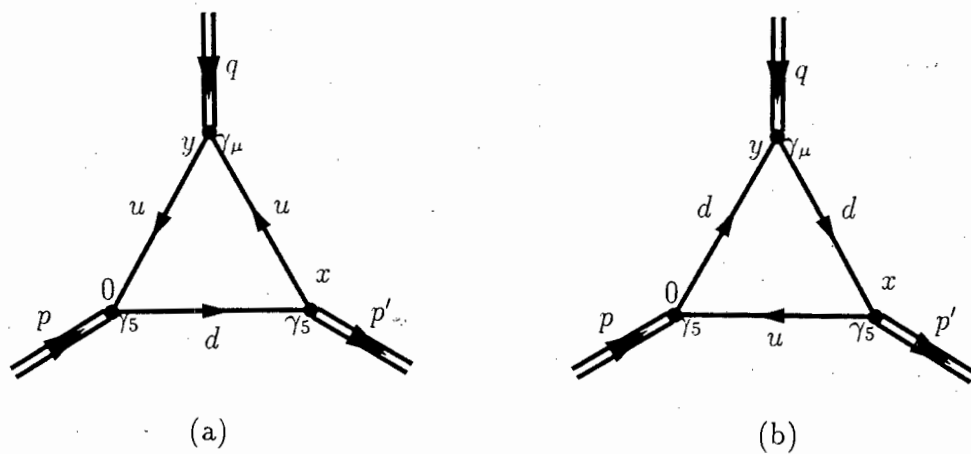


Figure 5.2: Graphical representation of the lowest order QCD contribution to $g_{\rho\pi\pi}$.

with

$$\text{Disc}\Pi(p^2, p'^2) = (-2i)^2 \text{Im}\Pi(p^2, p'^2) \quad (5.10)$$

From expression 5.7 by using equation 5.10 and the integrals evaluated in [52] (pag 29), $\text{Im}\Pi_\mu(q)$ becomes:

$$\text{Im}\Pi_\mu(q)|_{QCD} = \frac{3}{4\lambda^{\frac{3}{2}}}(m_u + m_d)^2 \left\{ q^2 s s' P_\mu + s s' q_\mu (s - s') \right\} \quad (5.11)$$

where the following notation was used:

$$\lambda = \left\{ s + s' - q^2 \right\}^2 - 4s s' ; p^2 = s ; p'^2 = s' ;$$

According to the philosophy of QCD sum rules, it is assumed that for s and s' values above the continuum thresholds (s_o and s'_o) the hadronic spectral function can be expressed in terms of QCD degrees of freedom.

$$\text{Im}\Pi(s, s', q^2)|_{HAD} = \text{RESONANCE PART} + \text{CONTINUUM} \quad (5.12)$$

$$\text{Im}\Pi(s, s', q^2)|_{HAD} = \text{RESONANCE PART} + \theta(s - s_o)\theta(s - s'_o) \text{Im}\Pi(s, s', q^2)|_{QCD} \quad (5.13)$$

The continuum is supposed to be well approximated by the perturbative QCD 5.11. The hadronic part of the correlator may be obtained after saturation with the pion intermediate state. Expression 5.1 becomes:

$$\Pi_\mu(q) = i^2 \cdot \iint d^4x d^4y \exp(-iq \cdot y) \cdot \exp(ip' \cdot x) \times \quad (5.14)$$

$$\sum_{k_1} \sum_{k_2} \langle 0 | j_\pi^\dagger(x) | \pi(k_1) \rangle \langle \pi(k_1) | J_\mu^\rho(y) | \pi(k_2) \rangle \langle \pi(k_2) | j_\pi(0) | 0 \rangle$$

Inyoking PCAC (see [52]),

$$\langle 0 | j(0) | \pi^\pm \rangle = \sqrt{2} \cdot f_\pi \cdot \mu_\pi^2 \quad (5.15)$$

$$\langle 0 | j^\dagger(x) | \pi^\pm \rangle = \sqrt{2} \cdot f_\pi \cdot \mu_\pi^2 \cdot \exp(-ikx) \quad (5.16)$$

and using the current-field identity [56] :

$$j_\mu^a = \frac{M_\rho^2}{f_\rho} \rho_\mu^a \quad (5.17)$$

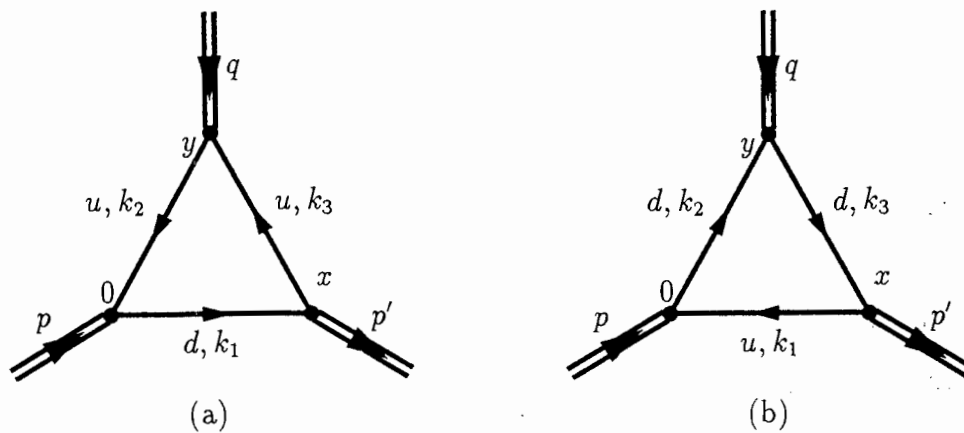


Figure 5.3: Graphical representation of the lowest order QCD contribution to $g_{\rho\pi\pi}$. The explicit momenta appear on each quark line.

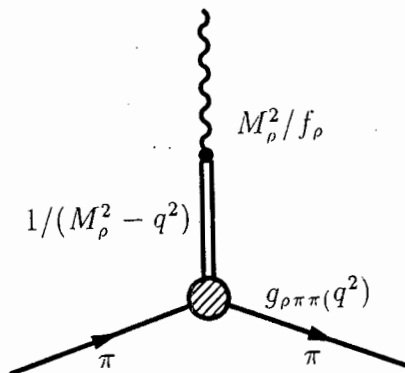


Figure 5.4: Rho-meson dominance diagram with the explicit coupling constants.

and VMD, one gets:

$$\langle \pi(k_1) | J_\mu^\rho | \pi(k_2) \rangle = -\frac{M_\rho^2}{f_\rho} \frac{1}{M_\rho^2 - q^2} (k_1 + k_2)_\mu \cdot g_{\rho\pi\pi}(q^2) \quad (5.18)$$

where j_μ^a is the isospin current ($a = 1, 2, 3$ is the isospin index), ρ_μ^a is the rho-meson field and μ_π is pion's mass. The experimental value of the coupling is $f_\rho = 5.0 \pm 0.1$, as obtained from the decay rate of the rho-meson into e^+e^- [50].

Being a function of q^2 , $g_{\rho\pi\pi}$ is a form factor. In the simpler version of VMD (single rho-meson dominance), the coupling would be strictly constant. Due to the radial excitations of the rho-meson (the $\rho(1450)$, $\rho(1700)$, etc.), which make a non-negligible contribution, $g_{\rho\pi\pi}$ becomes a form factor. The naive VMD applied to the electromagnetic pion form factor, for instance, predicts $g_{\rho\pi\pi}/f_\rho = 1$, while the experimental value is 20% higher. Hadronic models, such as the dual model [16], account for this difference by incorporating the rho-meson radial excitations. This gives $g_{\rho\pi\pi}(0)/f_\rho = 1$ but $g_{\rho\pi\pi}(M_\rho^2)/f_\rho \simeq 1.2$, in agreement with the experiment ($g_{\rho\pi\pi}(M_\rho^2) = 6.06 \pm 0.03$ according to [50]). At the same time, naive VMD does not fit the data too well in the spacelike region [16]. Much better fits are obtained by allowing a q^2 dependence of $g_{\rho\pi\pi}$.

Note that in addition to the pion contribution, there are additional terms from the pionic radial excitations (e.g. π' meson). These contributions are included in the hadronic continuum provided that the thresholds (continuum onsets) $s_o \simeq s'_o > 1 \div 3 \text{ GeV}^2$.

The hadronic part of $\Pi_\mu(q)$ proportional with $(p + p')_\mu$ becomes:

$$\Pi_\mu(q)|_{HAD} = -2f_\pi^2 \cdot \mu_\pi^4 \cdot g_{\rho\pi\pi}(Q^2) \cdot \frac{M_\rho^2}{f_\rho} \frac{(p + p')_\mu}{M_\rho^2 + Q^2} \frac{1}{(p^2 - \mu_\pi^2)} \frac{1}{(p'^2 - \mu_\pi^2)} \quad (5.19)$$

and :

$$\text{Im } \Pi_1(s, s', Q^2)|_{HAD} = -2f_\pi^2 \cdot \mu_\pi^4 \cdot \pi^2 \frac{g_{\rho\pi\pi}(Q^2)}{M_\rho^2 + Q^2} \cdot \frac{M_\rho^2}{f_\rho} \delta(s - \mu_\pi^2) \delta(s' - \mu_\pi^2) \quad (5.20)$$

with $Q^2 = -q^2 \geq 0$ and $f_\pi = 93.2 \text{ MeV}$.

The QCD-Hadron duality is, as before, implemented via Cauchy's theorem relation

1.3. The lowest dimensional FESR reads:

$$\int_0^{s_0} \int_0^{s'_0} \text{Im} \Pi_1(s, s') \Big|_{HAD} ds ds' = \int_0^{s_0} \int_0^{s'_0} \text{Im} \Pi_1(s, s') \Big|_{QCD} ds ds' \quad (5.21)$$

By substituting equations 5.11 and 5.19 in equation 5.21, the region of integration in the ss' plane is defined by the θ -functions in relation 5.13. It is reasonable to divide the ss' plane into three regions (see fig.5.5):

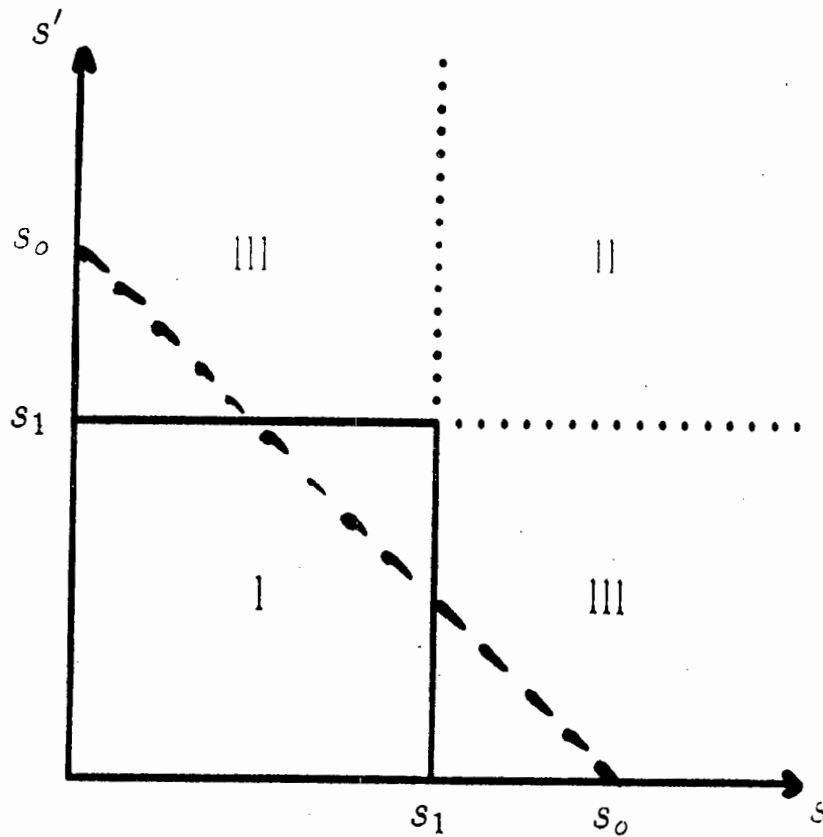


Figure 5.5: The integration region in the ss' plane. The solid and dashed lines are the boundaries of the integration region after the subtraction of the continuum in "square" and "triangle" versions.

Region I corresponds to the lowest resonance state contributions which are taken

into account explicitly. At large s, s' the contribution is determined by the quark loop of 5.2 (region II at a chosen sufficiently large value of s_1). In region III, only one of the variables s or s' is large. The contributions of quark states coincide with the contributions of real hadrons if they are averaged over some (equal) region of phase space. For not very large $Q^2 \leq s_o$, the contribution of region III is small [38]. The stability of the results relative to the chosen continuum model can be verified by considering another model, where the continuum contribution correspond to the region in fig. 5.5 separated from the origin by the dashed line. It turns out that different shapes for the integration region do not introduce appreciable differences in the numerical results (in fact for $s_o \simeq 1.5 \cdot s_1$ the results are practically the same in the both models).

Using for example the triangle shape of the integration region equation 5.21 becomes:

$$2\pi^2 \cdot f_\pi^2 \cdot \mu_\pi^4 \cdot g_{\rho\pi\pi}(Q^2) \frac{M_\rho^2}{f_\rho} \frac{1}{Q^2 + M_\rho^2} = \frac{3}{8} (m_u + m_d)^2 \frac{Q^2}{4} \int_0^{s_o} dx \int_{-x}^x dy \frac{x^2 - y^2}{\{(x+Q)^2 - x^2 + y^2\}^{3/2}} \quad (5.22)$$

where $s + s' = x$ ($x \in (0, s_o)$) and $s - s' = y$ ($y \in (-x, x)$). Evaluating analytically the integral appearing in equation 5.22 (using C.5), one gets:

$$\frac{g_{\rho\pi\pi}(Q^2)}{f_\rho} = \frac{3}{8\pi^2} \frac{f_\pi^2}{\langle \bar{q}q \rangle^2} \frac{Q^2}{M_\rho^2} (Q^2 + M_\rho^2) \cdot I(Q^2) \quad (5.23)$$

where

$$I(Q^2) = \frac{s_o}{16} \cdot \left(3 + \frac{s_o}{Q^2}\right) + \frac{1}{8} \left(s_o + \frac{3}{4}Q^2\right) \cdot \ln\left(\frac{Q^2}{Q^2 + 2s_o}\right) \quad (5.24)$$

The Gell-Mann Oakes Renner (GMOR) relation 4.1 was assumed.

According to Extended Vector Meson Dominance (EVMD) (i.e. VMD which allows a possible Q^2 dependence of $g_{\rho\pi\pi}$), the electromagnetic pion form factor is given by:

$$F_\pi(Q^2) \Big|_{EVMD} = \frac{M_\rho^2}{M_\rho^2 + Q^2} \frac{g_{\rho\pi\pi}(Q^2)}{f_\rho} \quad (5.25)$$

which becomes after the substitution of equation 5.23:

$$F_\pi(Q^2) \Big|_{EVMD} = \frac{3}{8\pi^2} \frac{f_\pi^2}{\langle \bar{q}q \rangle^2} \cdot Q^2 \cdot \left\{ \frac{s_o}{16} \cdot \left(3 + \frac{s_o}{Q^2}\right) + \frac{1}{8} \left(s_o + \frac{3}{4}Q^2\right) \cdot \ln\left(\frac{Q^2}{Q^2 + 2s_o}\right) \right\} \quad (5.26)$$

The determination of the electromagnetic pion form factor obtained from a three-point function involving the electromagnetic current and two axial-vector currents ([38] and [48]), which projects the form factor directly, making no use of VMD, gives:

$$F_{\pi}(Q^2)|_{EVMD} = \frac{1}{16\pi^2} \frac{1}{f_{\pi}^2} \frac{s'_o}{(1 + Q^2/2s'_o)^2} \quad (5.27)$$

Although equations 5.26 and 5.27 look structurally very different, they are numerically very similar for $Q^2 \geq 0.5 \text{ GeV}^2$, if $s_o \simeq 2.18 \text{ GeV}^2$, and $s'_o \simeq 1 \text{ GeV}^2$. The latter value leads to a very good fit of the data above 1 GeV^2 [38] and [48]. Although $s_o \simeq 2.18 \text{ GeV}^2$ seems a high value, $\sqrt{s_o} \simeq 1.47 \text{ GeV}$ is well inside the resonance region.

Also, the extrapolation of 5.23 to $Q^2 = 0$, for $s_o \simeq 2.18 \text{ GeV}^2$, gives $g_{\rho\pi\pi}(Q^2)/f_p \simeq 1$. Since the correlators are different, the onset of continuum need not to be the same in the two different cases. All one knows is that s_o and s'_o should roughly be in the region where the resonances loose prominence and the continuum takes over, somewhere in the interval $1 \div 3 \text{ GeV}^2$. The extrapolation to $Q^2 = 0$, of any of the above results should not be taken too seriously, as the OPE, the backbone of QCD sum rules diverges.

The good numerical agreement between equations 5.26 and 5.27 are shown in fig.5.6, that may be seen as a reflection of the validity of EVMD.

The experimental data used in fig. 5.6 are from [4].

5.3 $g_{\rho\pi\pi}$ at finite temperature

As we have seen in 3.23, at finite temperature, the fermion propagators develop a temperature correction, a term containing a Fermi factor. To derive an expression for $g_{\rho\pi\pi}$ at finite temperature, one should follow the same steps as in the zero temperature case, the operators being this time replaced by their thermal averages.

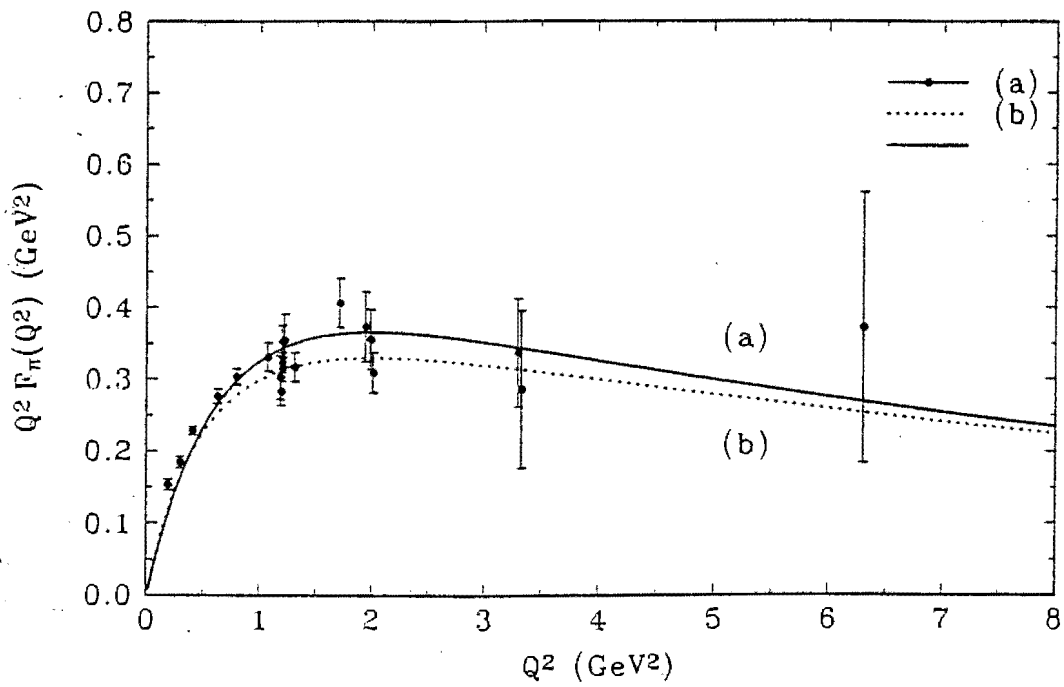


Figure 5.6: Showing the electromagnetic pion form factor at $T = 0$, determined from the QCD-FESR without invoking VMD- curve (a)-compared with the result of the independent QCD-FESR for $g_{\rho\pi\pi}$ plus VMD- curve (b).

By analogy with 5.5,

$$\begin{aligned} \Pi_\mu(q, T) &= \frac{i}{2} N_c (m_u + m_d)^2 \cdot \\ & \text{Tr} \left\{ \iint d^4x d^4y \exp(-iq \cdot y) \cdot \exp(ip' \cdot x) \int \frac{d^4k_1}{(2\pi)^4} \int \frac{d^4k_2}{(2\pi)^4} \int \frac{d^4k_3}{(2\pi)^4} \cdot \right. \\ & [\exp(-ik_1 \cdot x) \exp(ik_2 \cdot y) \cdot \exp(-ik_3(y-x)) \cdot \gamma_5 \cdot S(k_1, T) \cdot \gamma_5 \cdot S(k_2, T) \cdot \gamma_\mu \cdot S(k_3, T) - \\ & \left. \exp(ik_1 \cdot x) \exp(-ik_2 \cdot y) \cdot \exp(-ik_3(x-y)) \cdot \gamma_5 \cdot S(k_3, T) \cdot \gamma_\mu \cdot S(k_2, T) \cdot \gamma_5 \cdot S(k_1, T)] \right\} \end{aligned} \quad (5.28)$$

with $N_c = 3$ (the number of colours) and k_1 , k_2 and k_3 the same as those used in equation 5.5.

The diagrams in fig 5.7 show the various terms in $\Pi_\mu(q, T)$.

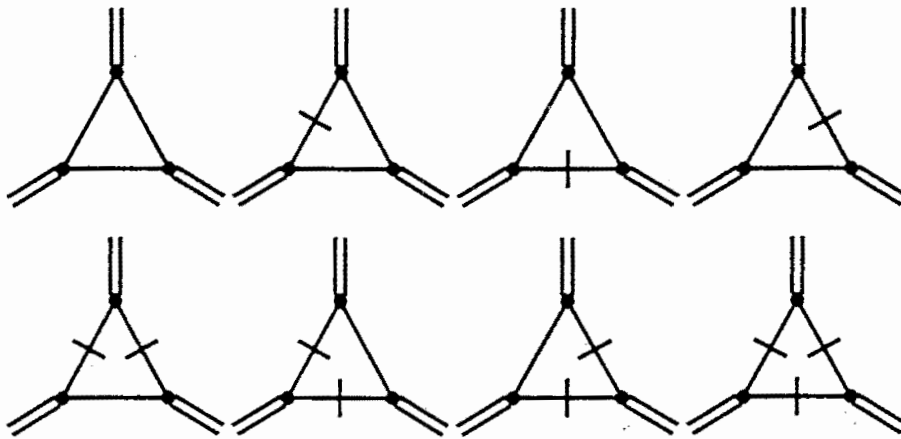


Figure 5.7: The first order loop diagrams contributing to $\Pi(q, T)$. In the diagrams, a straight internal quark line indicates a zero temperature propagator and a line with a slash through it indicates a quark propagator with the thermal insertion.

The first diagram corresponds to the zero temperature term $\Pi_\mu(q, 0) = \Pi_\mu(q)$; the next diagrams represent the temperature corrections (3 diagrams containing one Fermi factor each—a thermal insertion along one of the internal legs, the next 3 diagrams containing two Fermi factors each—one thermal insertion along two of the

internal legs and the last one contains three Fermi factors¹).

$\Pi_\mu(q, T)$ becomes:

$$\begin{aligned} \Pi_\mu(q, T) &= \frac{i}{2} N_c (m_u + m_d)^2 \cdot \\ &\left\{ \text{Tr}(\gamma_5 \gamma_\alpha \gamma_5 \gamma_\beta \gamma_\mu \gamma_\gamma) \int \frac{d^4 k}{(2\pi)^4} S^\alpha(k, T) \cdot S^\beta(k - p, T) \cdot S^\gamma(k - p', T) - \right. \\ &\left. - \text{Tr}(\gamma_5 \gamma_\alpha \gamma_\mu \gamma_\beta \gamma_5 \gamma_\gamma) \int \frac{d^4 k}{(2\pi)^4} S^\alpha(k + p', T) \cdot S^\beta(k + p, T) \cdot S^\gamma(k, T) \right\} \end{aligned} \quad (5.29)$$

Defining

$$I_1^{\alpha\beta\gamma}(T) = \int \frac{d^4 k}{(2\pi)^4} S^\alpha(k, T) \cdot S^\beta(k - p, T) \cdot S^\gamma(k - p', T), \quad (5.30)$$

one gets:

$$\begin{aligned} I_1^{\alpha\beta\gamma}(T) &= \int \frac{d^4 k}{(2\pi)^4} k^\alpha \cdot (k - p)^\beta \cdot (k - p')^\gamma \cdot \left\{ \left[\frac{1}{(k - p)^2} + 2\pi i \cdot n_F(|k_o - p_o|) \cdot \delta((k - p)^2) \right] \right. \\ &\quad \left. \left[\frac{1}{k^2} + 2\pi i \cdot n_F(|k_o|) \cdot \delta(k^2) \right] \cdot \left[\frac{1}{(k - p')^2} + 2\pi i \cdot n_F(|k_o - p'_o|) \cdot \delta((k - p')^2) \right] \right\} \end{aligned} \quad (5.31)$$

where $n_F(|k|)$ is the Fermi thermal factor defined in equation 3.23.

Similarly, because

$$\begin{aligned} S^\alpha(k + p', T) \cdot S^\beta(k + p, T) \cdot S^\gamma(k, T) &\underset{k \rightarrow -k}{=} -S^\alpha(k - p', T) \cdot S^\beta(k - p, T) \cdot S^\gamma(k, T) \\ I_2^{\alpha\beta\gamma}(T) &= - \int \frac{d^4 k}{(2\pi)^4} S^\alpha(k + p', T) \cdot S^\beta(k + p, T) \cdot S^\gamma(k, T) \end{aligned} \quad (5.32)$$

$$\begin{aligned} I_2^{\alpha\beta\gamma}(T) &= \int \frac{d^4 k}{(2\pi)^4} (k - p')^\alpha \cdot (k - p)^\beta \cdot k^\gamma \cdot \left\{ \left[\frac{1}{(k - p')^2} + 2\pi i \cdot n_F(|k_o - p'_o|) \cdot \delta((k - p')^2) \right] \right. \\ &\quad \left. \left[\frac{1}{(k - p)^2} + 2\pi i \cdot n_F(|k_o - p_o|) \cdot \delta((k - p)^2) \right] \cdot \left[\frac{1}{k^2} + 2\pi i \cdot n_F(|k_o|) \cdot \delta(k^2) \right] \right\} \end{aligned} \quad (5.33)$$

These lead to the following expression for the imaginary part of, for example $\Pi_1(q, T)$:

$$\text{Im} \Pi_1(s, s', Q^2, T) = \text{Im} \Pi_1(s, s', Q^2, 0) \cdot F(s, s', Q^2, T) \quad (5.34)$$

¹The thermal correction to $\Pi_\mu(q)$ containing three Fermi factors is real, i.e has no imaginary part.

with

$$F(s, s', Q^2, T) = 1 - n_1 - n_2 - n_3 + n_1 n_2 + n_1 n_3 + n_2 n_3 \quad (5.35)$$

where

$$n_1 = n_2 = n_F \left(\left| \frac{1}{2} \sqrt{\frac{x+y}{2}} \right| \right) \quad (5.36)$$

and

$$n_3 = n_F \left(\left| \frac{1}{2} \frac{Q^2 + \frac{x-y}{2}}{\sqrt{2(x+y)}} \right| \right) \quad (5.37)$$

Appendix D.2 provides a few more detailed steps that must be followed to get equation 5.35.

On the hadronic side, both f_π and $\langle \bar{q}q \rangle$ will develop a temperature dependence, and so will do s_o . The small variations of the rho-meson mass $M_\rho(T)$, can be safely ignored. This is not necessarily in contradiction with Kawarabayashi-Suzuki-Riazuddin-Fayyazuddin (KSRF) relation (see [26]) because even at $T = 0$ this relation has no rigorous justification (as it implies a massless ρ meson). The temperature corrections to KSRF relation are not known.

The modest increase in the vicinity of T_c , as obtained from QCD sum rules ([15]) and from other methods ([24]) does not change qualitatively the conclusions. Making use of equation 4.28 together with the results for $f_\pi(T)$ and $\langle \bar{q}q \rangle_T$ (in the chiral limit as well as for $m_q \neq 0$), and invoking the Gell-Mann Oakes Renner (GMOR) relation 4.1 at finite temperature (which only gets modified at next to leading order in the quark masses), the $T \neq 0$ FESR now, by analogy with equation 5.23, reads:

$$\frac{g_{\rho\pi\pi}(Q^2, T)}{f_\rho} = \frac{3}{8\pi^2} \frac{f_\pi^2(T)}{\langle \bar{q}q \rangle_T} \frac{Q^2}{M_\rho^2} (Q^2 + M_\rho^2) \cdot I(Q^2, T) \quad (5.38)$$

where

$$I(Q^2, T) = \frac{1}{8} \int_0^{s_o(T)} dx \int_{-x}^x dy \frac{(x^2 - y^2)}{(Q^4 + 2xQ^2 + y^2)^{3/2}} \cdot F(s, s', Q^2, T) \quad (5.39)$$

The integration cannot be done analytically, as in the zero temperature case of equation 5.24, but has to be done numerically.

The results for the ratio $g_{\rho\pi\pi}(Q^2, T)/g_{\rho\pi\pi}(Q^2, 0)$, calculated in the chiral limit ($m_q = 0$), for two different values of Q^2 , are shown in fig.5.8. To compare the chiral limit

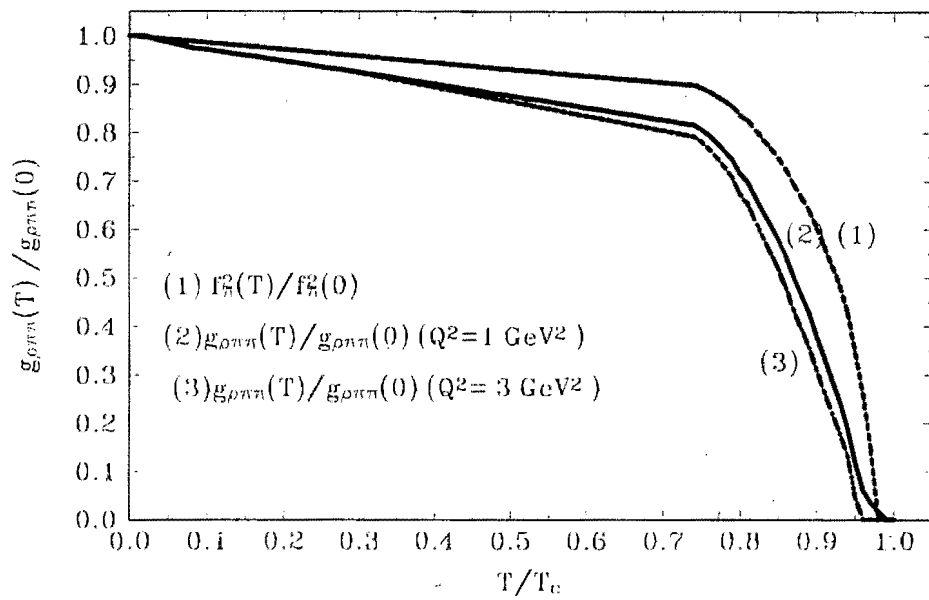


Figure 5.8: The ratio of the $\rho\pi\pi$ form factors at finite and zero temperature as functions of T/T_c . Both curves were obtained in chiral limit, but for different values of Q^2 .

results and $m_q \neq 0$ results, the ratio $g_{\rho\pi\pi}(Q^2, T)/g_{\rho\pi\pi}(Q^2, 0)$ as a function of temperature, was plotted for $Q^2 = 1 \text{ GeV}^2$. The comparison is depicted in fig.5.9.

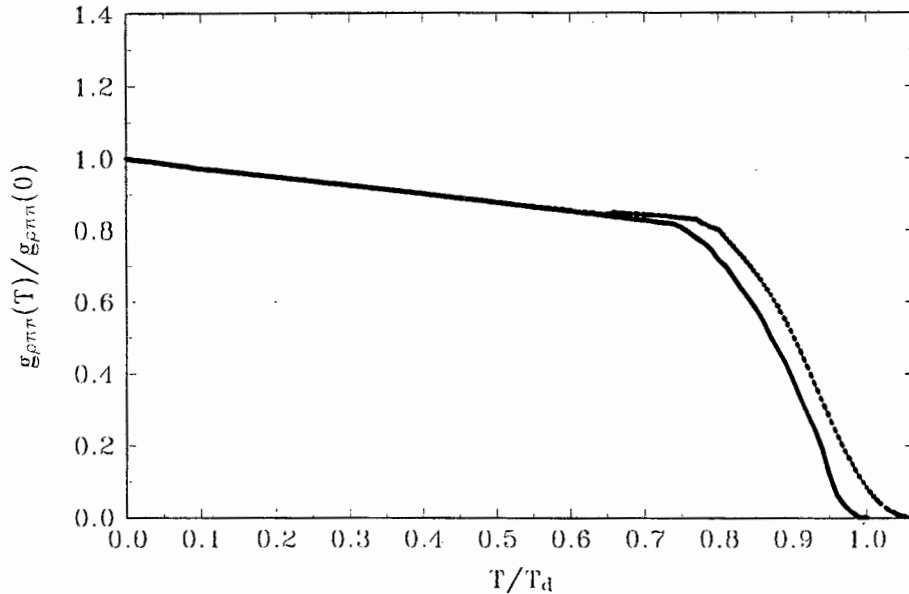


Figure 5.9: The ratio of the $\rho\pi\pi$ form factors at finite and zero temperatures as a function of T/T_c , for $Q^2 = 1 \text{ GeV}^2$. The solid line corresponds to the chiral limit calculations and the dotted line to calculations away from chiral limit.

Although $Q^2 = 1 \text{ GeV}^2$ was used in this figure, higher values of Q^2 give similar results.

It is important to remark that the vanishing of the ratio at or near the critical temperature, is basically Q^2 -independent, this providing analytical evidence for deconfinement.

The good agreement between the pion form factor using $g_{\rho\pi\pi}(Q^2)$ plus VMD and that obtained directly, without invoking VMD, persists at $T \neq 0$.

To see how $g_{\rho\pi\pi}$ varies with Q^2 for a certain temperature, $g_{\rho\pi\pi}$ was plotted against Q^2 . The result is given in fig.5.10.

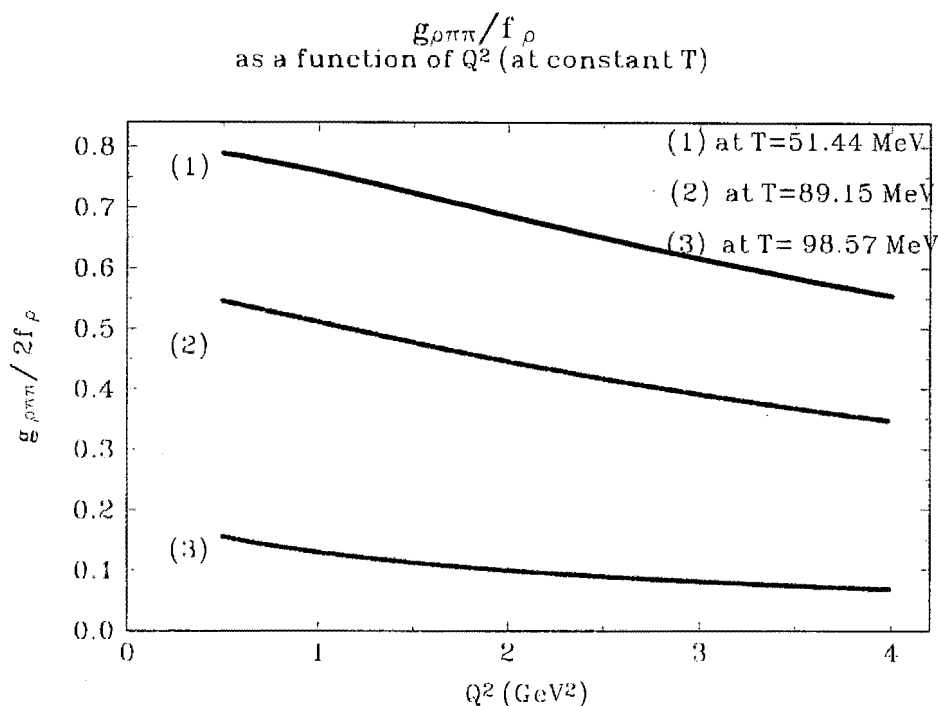


Figure 5.10: $g_{\rho\pi\pi}/f_\rho$ as a function of Q^2 , plotted for various constant temperatures.

Extrapolating the results from fig.5.10 to $Q^2 = 0$, one can see that $g_{\rho\pi\pi}(Q^2 = 0)/f_\rho$ is finite and decreases as the temperature increases.

5.4 The mean square pion radius

The same extrapolation to $Q^2 = 0$ from fig.5.10 allows the determination of the $\rho\pi\pi$ mean square radius, although the OPE breaks down at small values of Q^2 . The $\rho\pi\pi$ mean square radius is divergent at any temperature because of the mass singularities, but the ratio $\langle r^2 \rangle_T / \langle r^2 \rangle_0$ is well defined.

The $\rho\pi\pi$ mean square radius is defined as follows:

$$\langle r^2 \rangle_T = \frac{6}{g_{\rho\pi\pi}(0, T)} \left. \frac{\partial g_{\rho\pi\pi}(Q^2, T)}{\partial Q^2} \right|_{Q^2=0}$$

Using 5.38 :

$$\frac{g_{\rho\pi\pi}(Q^2, T)}{f_\rho} = \frac{3}{8\pi^2} \frac{f_\pi^2(T)}{\langle \bar{q}q \rangle_T^2} \frac{Q^2}{M_\rho^2} (Q^2 + M_\rho^2) \cdot I(Q^2, T)$$

where

$$I(Q^2, T) = \frac{1}{8} \int_0^{s_o(T)} dx \int_{-x}^x dy \frac{(x^2 - y^2)}{(Q^4 + 2xQ^2 + y^2)^{3/2}} \cdot F(s, s', Q^2, T),$$

for $T = 0$ one gets:

$$\langle r^2 \rangle_o = 6 \left\{ \frac{1}{M_\rho^2} + \frac{9/2 + 2 \ln(Q^2/2s_o)}{s_o} \right\} \quad (5.40)$$

As

$$\frac{\partial F}{\partial Q^2} = \frac{1}{T\sqrt{2(x+y)}} \cdot n_3 \cdot (n_3 - 1) \cdot (2n_1 - 1) \quad (5.41)$$

$\langle r^2 \rangle_T / \langle r^2 \rangle_o$ can be evaluated. Q^2 cannot be taken exactly zero, due to numerics, but for Q^2 small, after numerical integration (Gaussian integration routine here), a graph of $\langle r^2 \rangle_T / \langle r^2 \rangle_o$ against T/T_c was obtained. The result appears in fig.5.11. The ratio of quantities which have mass singularities is well defined. By changing Q^2 over a wide range in the vicinity of $Q^2 = 0$, results remain basically unchanged. Thus, the ratio should be well behaved at zero momentum.

$\langle r^2 \rangle_T / \langle r^2 \rangle_o$ increases with increasing T until the critical temperature, where it becomes infinite, signalling thus, the deconfinement, as one could have expected from an intuitive point of view. Other values of Q^2 , close to $Q^2 = 0$ give the same results.

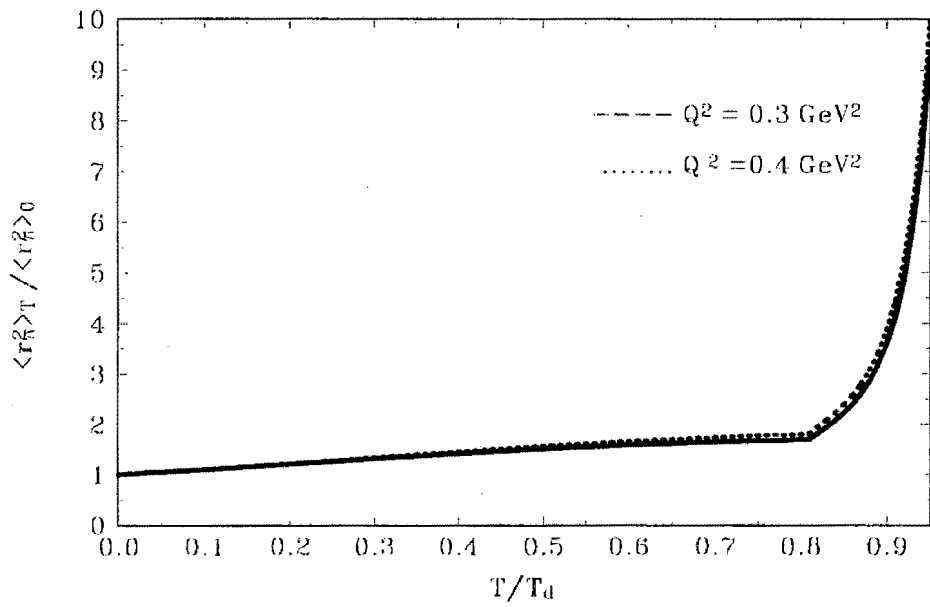


Figure 5.11: The ratio of the (strong) pion radius at finite and at zero temperatures as a function of T/T_c . The solid line corresponds to $Q^2 = 0.3 \text{ GeV}^2$ and the dashed line corresponds to $Q^2 = 0.4 \text{ GeV}^2$.

Chapter 6

Conclusion

6.1 Conclusion

The investigation of the current algebra Gell-Mann, Oakes and Renner relation at non-zero temperature, in the framework of QCD sum rules found no corrections at leading order in the quark masses. At the next to leading order, corrections of the form $m_q^2 \cdot T^2$ were found, but these are small except near the critical temperature.

The first two lowest order FESR sum rules were used to determine the temperature dependence of the pion mass. $\mu_\pi(T)$ is essentially constant, except very close to T_c , where it increases with the temperature. The results obtained using the two different order sum rules are in good agreement one with the other, and with a variety of independent determinations in different frameworks [3],[13], [30], [40], [57].

Finite Energy QCD sum rules (FESR) at $T \neq 0$, for a three point function involving the rho-meson interpolating current plus two axial-vector divergencies were used. The Q^2 and T dependence of the $\rho\pi\pi$ coupling and the validity of Vector Meson Dominance at finite temperature were investigated.

The pion form factor $g_{\rho\pi\pi}(Q^2)$ at zero temperature, determined from sum rules together with VMD, was compared with the experimental data on the pion form factor and also with a direct determination, i.e. with a theoretical result not relying on VMD. The very good fit at $T = 0$ was taken as a evidence in the support of VMD at zero temperature. In the absence of experimental data at $T \neq 0$, the agreement

between the two theoretical results (sum rules together with VMD and the direct determination), was taken as evidence in support of VMD at finite temperature.

The plot of the ratio $g_{\rho\pi\pi}(Q^2, T)/g_{\rho\pi\pi}(Q^2, 0)$ as a function of T/T_c in the chiral limit ($m_q = 0$) case, indicated the vanishing of the ratio at the critical temperature. The same shape of the plots for different Q^2 ($Q^2 = 1 \text{ GeV}^2$ and $Q^2 = 3 \text{ GeV}^2$, in this case), is a indication that the vanishing of the ratio at the critical temperature is basically Q^2 -independent, providing analytical evidence for deconfinement. The plot of the ratio $g_{\rho\pi\pi}(Q^2, T)/g_{\rho\pi\pi}(Q^2, 0)$ as a function of temperature, for $Q^2 = 1 \text{ GeV}^2$ comparing chiral limit results ($m_q = 0$) and away from chiral limit results ($m_q \neq 0$) provided again, analytical evidence for deconfinement.

The extrapolation of $g_{\rho\pi\pi}(Q^2)/f_\rho$ vs Q^2 graph for three different temperatures, to $Q^2 = 0$ proved that $g_{\rho\pi\pi}(Q^2 = 0)/f_\rho$ is finite and decreases as the temperature increases. The same extrapolation to $Q^2 = 0$ allowed the determination of the $\rho\pi\pi$ mean square radius. Even if the $\rho\pi\pi$ mean square radius is divergent at any temperature because of the mass singularities the ratio $\langle r^2 \rangle_T / \langle r^2 \rangle_0$ is well defined. $\langle r^2 \rangle_T / \langle r^2 \rangle_0$ increases with increasing T until the critical temperature, where it becomes infinite, signalling thus, the deconfinement.

The increase in the pion mass around T_c does not contradict the image that pions, rho-mesons etc. should be absent from QGP as the mass of a particle is not an order parameter for deconfinement. Rather it is the imaginary part of the propagator, i.e. it's width, which signal the deconfinement.

All these are consistent with one's expectations that for temperatures exceeding the critical temperatures, the pion will cease to exist.

6.2 Critical Assessment of the QCD Sum-Rule Approach

After all this discussion, the place the Sum Rules method occupies in the catalog of the existing approaches to hadronic physics should be specified.

The QCD sum-rule approach to hadronic properties is now rather mature. Sum-rule methods have produced phenomenological successes for a wide range of problems, some far beyond the original application of meson masses and couplings.

Despite the popularity and apparent success of QCD sum-rules, there remain concerns about the validity of various aspects of the approach. The sum rule method is admittedly approximate. It requires a certain amount of guesswork and cannot be formalized in the same sense as, say, the solution of the Schrödinger equation. At the same time, it is not a model because any model requires ad hoc assumptions and the accuracy of the corresponding predictions can not be controlled inside the model itself. In the sum rule method, once the rules of the game are accepted (the condensates are introduced once and forever) there is no freedom left.

The nature of the sum-rule approach should be taken into account when accessing the value of its predictions. It is not the quantitative predictions for hadron masses and other properties that are the most important. Far more precise determinations of the hadronic spectrum will ultimately be provided by the lattice calculations. It is the quantitative relations and the qualitative insight that are the most valuable, and which will persist to challenge numerical or model predictions.

It has been said that QCD sum-rules work well only when making "postdictions" rather than predictions. One can say that the reliability of sum-rule approach, particularly when applied to new observables and new domains, is not guaranteed without some feedback from experiment. The usefulness of postdictions should not be underestimated. After all, the data is provided by the experiment and what we seek is understanding how it fits into a larger picture. This is what the sum rules can provide.

Acknowledgements

I received great amounts of encouragement, support and help from many people during my studies. My most sincere thanks go to all of them.

I would like to thank my supervisor, Professor C.A. Dominguez for his guidance, encouragement, expert advice and patience throughout my Ph.D studies.

I am grateful to the Foundation for Research and Development for financial support, in the form of FRD bursaries during the past three years.

The staff and the postgraduate students from Physics Department deserve mention for all the helpful discussions about Physics (and not only) I had with them.

Many people outside the Physics community have given me support and encouragement; my warmest thanks to all these friends.

I would like to thank Dr.G.C.Paunescu, who's financial support helped this thesis come to life. Thanks for the trust and encouragement you offered me when I needed them most.

My hearty thanks to my parents for their unconditional love, constant support, encouragement and understanding.

Most of all, I would like to thank my husband, Remus, who's love, understanding, patience and encouragement has been a constant source of inspiration and energy for me. Thanks for the many discussions and critical comments we had about physics, analysis, computing or statistics that undoubtedly helped my research, and thanks for reading all the versions of this thesis.

Appendix A

Generalities

A.1 Notations and conventions

Unless otherwise stated, the natural units $\hbar = c = 1$ were used. $\hbar = \frac{h}{2\pi}$ where h is the Planck constant and c the velocity of light in vacuum. In these units mass, momentum and energy are measured in GeV and length and time are measured in units of GeV^{-1} .

Some useful conversion factors:

$$1 \text{ kg} \qquad \qquad \qquad \doteq 5.61 \times 10^{26} \text{ GeV}$$

$$1 \text{ m} \qquad \qquad \qquad = 5.07 \times 10^{15} \text{ GeV}^{-1}$$

$$1 \text{ s} \qquad \qquad \qquad = 1.52 \times 10^{24} \text{ GeV}^{-1}$$

$$1 \text{ fermi} = 1 \text{ F} = 10^{-13} \text{ cm} \quad = 5.07 \text{ GeV}^{-1}$$

$$(1 \text{ F})^2 \qquad \qquad \qquad = 10 \text{ mb}$$

$$(1 \text{ GeV})^{-2} \qquad \qquad \qquad = 0.389 \text{ mb}$$

where mb denotes the unit for cross-sections: $1 \text{ mb (millibarn)} = 10^{-27} \text{ cm}^2$.

A.2 γ -Algebra

The γ matrices are taken to be of dimension D (4). There are D γ^μ matrices:

$$\gamma^0, \gamma^1, \gamma^2, \dots, \gamma^{D-1}$$

and a matrix γ^5 .

For $D = 4$:

$$\gamma^0 = \begin{pmatrix} I & 0 \\ 0 & -I \end{pmatrix}; \gamma^k = \begin{pmatrix} 0 & \sigma^k \\ -\sigma^k & 0 \end{pmatrix}$$

where σ^k are the 2×2 Pauli matrices:

$$\sigma^1 = \begin{pmatrix} 0 & 1 \\ 1 & 0 \end{pmatrix}; \sigma^2 = \begin{pmatrix} 0 & -i \\ i & 0 \end{pmatrix}; \sigma^3 = \begin{pmatrix} 1 & 0 \\ 0 & -1 \end{pmatrix};$$

They verify the anticommutation relations:

$$\{\gamma^\mu, \gamma^\nu\} = 2g^{\mu\nu}, \gamma^5 = i\gamma^0\gamma^1\gamma^2\dots\gamma^{D-1} = \gamma_5; (\gamma^5)^2 = 1 \quad (\text{A.1})$$

$$\gamma^\mu\gamma^5 + \gamma^5\gamma^\mu = 0 \quad (\text{A.2})$$

with

$$\left\{ \begin{array}{l} g^{\mu\nu} = 0, \mu \neq \nu \\ g^{00} = 1 \\ g^{ii} = -1, \text{ for } i = 1, \dots, D-1 \end{array} \right. \quad (\text{A.3})$$

$$g^{\mu\nu} = g_{\mu\nu}; \quad (\text{A.4})$$

$$g^{\mu\nu}g_{\mu\nu} = 4 \quad (\text{A.5})$$

$$g^{\mu\nu}\delta_{\mu\nu} = \begin{cases} -2 & (\text{Minkowski}) \\ 4 & (\text{Euclidian}) \end{cases} \quad (\text{A.6})$$

$$\gamma^\mu\gamma_\mu = 4 \quad (\text{A.7})$$

$$\gamma^\mu\gamma^\nu\gamma_\mu = -2\gamma^\nu \quad (\text{A.8})$$

$$\gamma^\mu\gamma^\alpha\gamma^\beta\gamma_\mu = 4g^{\alpha\beta} \quad (\text{A.9})$$

$$\gamma^\mu\gamma^\alpha\gamma^\beta\gamma^\rho\gamma_\mu = -2\gamma^\rho\gamma^\beta\gamma^\alpha \quad (\text{A.10})$$

$$(\gamma^5)^\dagger = \gamma^5 \quad (\text{A.11})$$

$$(\gamma^\mu)^\dagger = \gamma_\mu = \begin{cases} \gamma_\mu & \mu = 0 \\ -\gamma^\mu & \mu \neq 0 \end{cases} \quad (\text{A.12})$$

$$(\gamma_\mu)^\dagger = \gamma_0\gamma_\mu\gamma_0 \quad (\text{A.13})$$

$$\text{Tr}(\gamma_\mu\gamma_\nu) = 4g_{\mu\nu} \quad (\text{A.14})$$

$$\text{Tr}(\gamma_\mu\gamma_\nu\gamma_\sigma\gamma_\lambda) = 4(g_{\mu\nu}g_{\sigma\lambda} + g_{\mu\lambda}g_{\nu\sigma} - g_{\mu\sigma}g_{\nu\lambda}) \quad (\text{A.15})$$

$$\text{Tr}(\gamma_5) = \text{Tr}(\gamma_\mu\gamma_5) = \text{Tr}(\gamma_\mu\gamma_\nu\gamma_5) = \text{Tr}(\gamma_\mu\gamma_\nu\gamma_\sigma\gamma_5) = 0 \quad (\text{A.16})$$

$$\text{Tr}(\not{a}\not{b}) = 4a \cdot b \quad (\text{A.17})$$

$$\text{Tr}(\not{a}\not{b}\not{c}\not{d}) = 4[(a \cdot b)(c \cdot d) + (a \cdot d)(b \cdot c) - (a \cdot c)(b \cdot d)] \quad (\text{A.18})$$

A.3 Generators for the fundamental representation of $SU_c(3)$

For $SU_c(3)$, $t^a = \frac{1}{2}\lambda^a$ with:

$$\lambda^j = \begin{pmatrix} \sigma^j & 0 \\ 0 & 0 \end{pmatrix}; j = 1, 2, 3; \lambda^4 = \begin{pmatrix} 0 & 0 & 1 \\ 0 & 0 & 0 \\ 1 & 0 & 0 \end{pmatrix}; \lambda^5 = \begin{pmatrix} 0 & 0 & -i \\ 0 & 0 & 0 \\ i & 0 & 0 \end{pmatrix};$$

$$\lambda^6 = \begin{pmatrix} 0 & 0 & 0 \\ 0 & 0 & 1 \\ 0 & 1 & 0 \end{pmatrix}; \lambda^7 = \begin{pmatrix} 0 & 0 & 0 \\ 0 & 0 & -i \\ 0 & i & 0 \end{pmatrix}; \lambda^8 = \frac{1}{\sqrt{3}} \begin{pmatrix} 1 & 0 & 0 \\ 0 & 1 & 0 \\ 0 & 0 & -2 \end{pmatrix}; \quad (\text{A.19})$$

and:

$$[t^a, t^b] = i \sum f^{abc} t^c \quad (\text{A.20})$$

f are totally anti-symmetric. The only nonzero elements (up to permutations) are:

$$1 = f_{123} = 2f_{147} = 2f_{246} = 2f_{257} = 2f_{345} = -2f_{156} = -2f_{367} = \frac{2}{\sqrt{3}}f_{458} = \frac{2}{\sqrt{3}}f_{678} \quad (\text{A.21})$$

Appendix B

Currents and operators

The following set of currents, coupled to observed physical meson states have been studied:

$$j_S = \bar{q}_i q_j \quad J^{PC} = 0^{++}$$

$$j_P = i \cdot \bar{q}_i \gamma_5 q_j \quad J^{PC} = 0^{-+}$$

$$j_V = \bar{q}_i \gamma_\mu q_j \quad J^{PC} = 1^{--}$$

$$j_A = \eta_{\mu\nu} \bar{q}_i \gamma_\nu \gamma_5 q_j \quad J^{PC} = 1^{++}$$

$$j_{A'} = \bar{q}_i \partial_\mu \gamma_5 q_j \quad J^{PC} = 1^{+-}$$

$$j_T = i \cdot \bar{q}_i (\gamma_\mu \partial_\nu + \gamma_\nu \partial_\mu + \frac{2}{3} \eta_{\mu\nu} \partial) q_j \quad J^{PC} = 2^{++}$$

$$j_{T'} = i \cdot \bar{q}_i (\gamma_\mu \gamma_5 \partial_\nu + \gamma_\nu \gamma_5 \partial_\mu + \frac{2}{3} \eta_{\mu\nu} \gamma_5 \partial) q_j \quad J^{PC} = 2^{-+}$$

where $\eta_{\mu\nu}$ is a constant $\eta_{\mu\nu} = +1, -1, +i, -i$, defined by $\Gamma_\mu \Gamma_\nu = \eta_{\mu\nu} \Gamma_\rho$ (see section 1.2).

The first six dimension set of operators with zero spin used in OPE are the following:

$$I \quad d = 0$$

$$m \cdot \bar{q}q \quad d = 4$$

$$G_{\mu\nu}^a \cdot G_{\mu\nu}^a \quad d = 4$$

$$\bar{q}\Gamma_1 q \bar{q}\Gamma_2 q \quad d = 6$$

$$\tilde{m} \bar{q} \sigma_{\mu\nu} \frac{\lambda^a}{2} q G_{\mu\nu}^a \quad d = 6$$

$$f_{abc} G_{\mu\nu}^a G_{\nu\gamma}^b G_{\gamma\mu}^c \quad d = 6$$

where m and \tilde{m} are matrices in flavour space whose elements are proportional with quark masses, λ^a are Gell-Mann $SU(3)$ matrices, $Tr(\lambda^a \cdot \lambda^b) = 2\delta^{ab}$, $\sigma_{\mu\nu} = \frac{1}{2} \cdot i [\gamma_\mu, \gamma_\nu]$ and $G_{\mu\nu}^a$ is the gluon field tensor.

Appendix C

Dimensional regularization

An integral of a polynomial in k^μ times $f(k^2)$ can be reduced to an integral 2.12 by symmetrical integration:

$$\int d^D k f(k^2) k^\mu k^\nu = \frac{g^{\mu\nu}}{D} \int d^D k f(k^2) k^2; \quad (\text{C.1})$$

C.1 Feynman's parametrization

When the energy-momentum of an internal line in a Feynman diagram is not completely fixed, there is a non-trivial integration to be performed in four-dimensional space if one doesn't use the set of clever tricks invented by Feynman:

$$\frac{1}{a^\alpha b^\beta} = \frac{\Gamma(\alpha + \beta)}{\Gamma(\alpha)\Gamma(\beta)} \int_0^1 dx \frac{x^{\alpha-1} (1-x)^{\beta-1}}{[ax + b(1-x)]^{\alpha+\beta}} \quad (\text{C.2})$$

and

$$\frac{1}{a^\alpha b^\beta c^\gamma} = \frac{\Gamma(\alpha + \beta + \gamma)}{\Gamma(\alpha)\Gamma(\beta)\Gamma(\gamma)} \int_0^1 dx x \int_0^1 dy \frac{(xy)^{\alpha-1} [x(1-y)]^{\beta-1} (1-x)^{\gamma-1}}{[axy + (b-a)x + (c-a)y]^{\alpha+\beta+\gamma}} \quad (\text{C.3})$$

where α, β, γ are real numbers and $\Gamma(z)$ is the Euler gamma function:

$$\Gamma(z) = \int_0^\infty dt t^{z-1} \exp(-t); \text{Re } z > 0$$

$$\Gamma(z+1) = z\Gamma(z)$$

$$\Gamma(n+1) = n!; n \in Z$$

$$\Gamma\left(\frac{1}{2}\right) = \sqrt{\pi}$$

$$\Gamma(-\varepsilon) = -\frac{1}{\varepsilon} - \gamma;$$

where $\gamma = 0.577215\dots$ (Euler's constant)

C.2 Some integrals

Some of the ultraviolet divergent (undefined) integrals appearing during the calculations, can be evaluated using C.2 and C.3. For example:

$$I = \int \frac{d^D k}{(2\pi)^D} \frac{1}{k^2(k-q)^2}; D = 4 + 2\varepsilon$$

$$I = \int \frac{d^D k}{(2\pi)^D} \frac{\Gamma(4)}{\Gamma(2)\Gamma(2)} \int_0^1 dx \frac{1}{[(k-q)^2 x + k^2(1-x)]^4} =$$

$$6 \int_0^1 dx \int \frac{d^D k}{(2\pi)^D} \frac{1}{[(k-q)^2 x + k^2(1-x)]^4} = 6 \int_0^1 dx \int \frac{d^D k}{(2\pi)^D} \frac{1}{[(k-qx)^2 + q^2 x(1-x)]^4}$$

using the fact that

$$\int \frac{d^D k}{(2\pi)^D} \frac{(k^2)^\alpha}{[k^2 - a^2]^\beta} = \frac{i(-a^2)^{\alpha-\beta+2}}{(4\pi)^2} \left(\frac{a^2}{4\pi}\right)^\varepsilon \frac{\Gamma(2+\alpha+\varepsilon)\Gamma(\beta-\alpha-2-\varepsilon)}{\Gamma(\beta)\Gamma(2+\varepsilon)}; D = 4+2\varepsilon \quad (C.4)$$

$$I = 6\Gamma(-\varepsilon) \int_0^1 dx \cdot \left[\frac{-q^2 x(1-x)}{4\pi} \right]^\varepsilon$$

in the limit $\varepsilon \rightarrow 0$

$$I = \int \frac{d^D k}{(2\pi)^D} \frac{1}{k^2(k-q)^2} = \frac{i}{(4\pi)^2} \left[-\frac{1}{\varepsilon} + \ln(4\pi) - \gamma - \int_0^1 dx \ln(q^2 x(1-x)) + \dots \right]$$

Using Appendix C.3:

$$I = \int \frac{d^D k}{(2\pi)^D} \frac{1}{k^2(k-q)^2} = \frac{i}{(4\pi)^2} \left[-\frac{1}{\varepsilon} + \ln(4\pi) - \gamma - \ln\left(-\frac{q^2}{\nu^2}\right) + 2 \right] \quad (C.5)$$

For convenience $D \rightarrow 4$ is understood and the singular terms are dropped.

Similarly it can be proved that :

$$I^\alpha = \int \frac{d^4 k}{(2\pi)^4} \frac{k^\alpha}{k^2(k-q)^2} = -\frac{i}{(4\pi)^2} \frac{q^\alpha}{2} \left[\ln\left(-\frac{q^2}{\nu^2}\right) - 2 \right] \quad (C.6)$$

$$\begin{aligned}
I^{\alpha\beta} &= \int \frac{d^4k}{(2\pi)^4} \frac{k^\alpha k^\beta}{k^2(k-q)^2} \\
&= \frac{i}{(4\pi)^2} \left[q^2 g^{\alpha\beta} \left(\frac{1}{12} \ln \left(-\frac{q^2}{\nu^2} \right) - \frac{2}{9} \right) + q^\alpha q^\beta \left(-\frac{1}{3} \ln \left(-\frac{q^2}{\nu^2} \right) + \frac{13}{18} \right) \right]
\end{aligned} \tag{C.7}$$

$$\begin{aligned}
I &= \int \frac{d^4k}{(2\pi)^4} \frac{1}{k^2 [(k-q)^2 - m^2]} \\
&= -\frac{i}{(4\pi)^2} \left[\ln \left(-\frac{q^2}{\nu^2} \right) + \frac{m^2}{q^2} \ln \left(-\frac{m^2}{q^2} \right) + \left(1 - \frac{m^2}{q^2} \right) \ln \left(1 - \frac{m^2}{q^2} \right) - 2 \right]
\end{aligned} \tag{C.8}$$

$$\begin{aligned}
I^\alpha &= \int \frac{d^4k}{(2\pi)^4} \frac{k^\alpha}{k^2 [(k-q)^2 - m^2]} \\
&= -\frac{i q^\alpha}{2(4\pi)^2} \left\{ \ln \left(-\frac{q^2}{\nu^2} \right) + \frac{m^2}{q^2} \left(2 - \frac{m^2}{q^2} \right) \ln \left(-\frac{m^2}{q^2} \right) + \right. \\
&\quad \left. \left(1 - 2\frac{m^2}{q^2} + \frac{m^4}{q^4} \right) \ln \left(1 - \frac{m^2}{q^2} \right) + \frac{m^2}{q^2} - 2 \right\}
\end{aligned} \tag{C.9}$$

$$\begin{aligned}
I &= \int \frac{d^4k}{(2\pi)^4} \frac{1}{(k^2 - m^2) [(k-q)^2 - m^2]} \\
&= -\frac{i}{(4\pi)^2} \left[\ln \left(\frac{m^2}{\nu^2} \right) + \sqrt{1 - 4\frac{m^2}{q^2}} \ln \frac{\sqrt{1 - 4\frac{m^2}{q^2}} + 1}{\sqrt{1 - 4\frac{m^2}{q^2}} - 1} - 2 \right]
\end{aligned} \tag{C.10}$$

C.3 Logarithmic integrals:

For

$$I_n = \int_0^1 dx x^n \ln(u - x(1-x)) \tag{C.11}$$

one gets:

$$I_o = -2 + \ln u + \sqrt{1-4u} \ln \frac{\sqrt{1-4u} + 1}{\sqrt{1-4u} - 1} \tag{C.12}$$

$$I_1 = \frac{1}{2} I_o \tag{C.13}$$

$$I_2 = \frac{1}{3} \left\{ -\frac{13}{6} + 2u + \ln u + (1-u) \sqrt{1-4u} \ln \frac{\sqrt{1-4u} + 1}{\sqrt{1-4u} - 1} \right\} \tag{C.14}$$

$$I_3 = \{I_o - 3I_1 + 3I_2\} \tag{C.15}$$

C.4 Integrals involving δ -functions

To evaluate

$$I = \int \frac{d^4 k}{(2\pi)^4} \delta^+(k^2 - m_u^2) \delta^+((k - q)^2 - m_d^2),$$

one can use the fact that:

$$\delta^+(k^2 - m_u^2) = \frac{1}{2|k_o|} \delta(k_o - \sqrt{|\vec{k}|^2 + m_u^2}).$$

I becomes:

$$I = \int \frac{d^3 k}{(2\pi)^4 \sqrt{|\vec{k}|^2 + m_u^2}} \delta^+ \left(\Delta m^2 + q^2 + 2|\vec{k}||\vec{q}|z - 2q_o \sqrt{|\vec{k}|^2 + m_u^2} \right)$$

where $k = (k_o, |\vec{k}|)$, $q = (q_o, |\vec{q}|)$, $\Delta m^2 = m_u^2 - m_d^2$, $z = \cos \theta$; with θ - being the angle between \vec{k} and \vec{q} .

But

$$\int d^3 k = 2\pi \int_{-1}^1 dz \int_0^\infty |\vec{k}|^2 d|\vec{k}|$$

and

$$\delta(f(z)) = \frac{\delta(z - z^*)}{|f'(z)|_{z=z^*}}$$

therefore:

$$I = \frac{2\pi}{2(2\pi)^4} \int_{-1}^1 dz \int_{\frac{q_o - |\vec{q}|}{2}}^{\frac{q_o + |\vec{q}|}{2}} d|\vec{k}| \delta(z - z^*) \frac{1}{2|\vec{q}|}$$

The limits of integration $\frac{q_o - |\vec{q}|}{2} \leq |\vec{k}| \leq \frac{q_o + |\vec{q}|}{2}$ are coming from the condition $-1 \leq z^* \leq 1$, therefore. The above leads to:

$$I = \frac{1}{(2\pi)^4} \frac{\pi}{2},$$

therefore:

$$I = \int \frac{d^4 k}{(2\pi)^4} \delta^+(k^2 - m_u^2) \delta^+((k - q)^2 - m_d^2) = \frac{1}{(2\pi)^4} \frac{\pi}{2} \quad (\text{C.16})$$

Similarly it can be proved that:

$$I^\alpha = \int \frac{d^4 k}{(2\pi)^4} k^\alpha \delta^+(k^2 - m_u^2) \delta^+((k - q)^2 - m_d^2) = \frac{q^\alpha}{2} \left(1 + \frac{\Delta m}{\nu}\right) I \quad (\text{C.17})$$

where $\Delta m = m_u - m_d$.

In $\text{Im } \Pi_5(q^2, T)$ from 4.19 the following integrals are involved:

$$I(T) = \int \frac{d^4 k}{(2\pi)^4} n_F(|k_o|) \delta(k^2) \delta^+((k-q)^2) \quad (\text{C.18})$$

$$I^\alpha(T) = \int \frac{d^4 k}{(2\pi)^4} k^\alpha n_F(|k_o|) \delta(k^2) \delta^+((k-q)^2) = \frac{q^\alpha}{2} I(T) \quad (\text{C.19})$$

$$I'(T) = \int \frac{d^4 k}{(2\pi)^4} n_F(|(k-q)_o|) \delta^+(k^2) \delta((k-q)^2) \quad (\text{C.20})$$

Let us compute them:

$$\begin{aligned} I(T) &= \frac{1}{2} \int \frac{d^4 k}{(2\pi)^4} n_F(|k_o|) \frac{1}{|\vec{k}|} \left[\delta(k_o - |\vec{k}|) + \delta(k_o + |\vec{k}|) \right] \delta^+((k-q)^2) \\ &= \int \frac{d^3 k}{2(2\pi)^4 |\vec{k}|} n_F(|\vec{k}|) \left\{ \delta(q^2 - 2q_o |\vec{k}| + 2|\vec{k}| |\vec{q}| z) + \delta(q^2 + 2q_o |\vec{k}| + 2|\vec{k}| |\vec{q}| z) \right\} \end{aligned}$$

where $k = (k_o, |\vec{k}|)$, $q = (q_o, |\vec{q}|)$, $q_o = \omega$, $\Delta m^2 = m_u^2 - m_d^2$, $z = \cos \theta$; with θ - being the angle between \vec{k} and \vec{q} .

Therefore:

$$I(T) = \frac{2\pi}{2(2\pi)^4} \int_{-1}^1 dz \int d|\vec{k}| \delta(z - z_1^*) \delta(z - z_2^*) \frac{1}{2|\vec{q}|} n_F(|\vec{k}|)$$

From the condition :

$$-1 \leq z_1^* \leq 1 \Rightarrow \frac{\omega - |\vec{q}|}{2} \leq |\vec{k}| \leq \frac{\omega + |\vec{q}|}{2}$$

and from the condition :

$$-1 \leq z_2^* \leq 1 \Rightarrow -\frac{\omega + |\vec{q}|}{2} \leq |\vec{k}| \leq -\frac{\omega - |\vec{q}|}{2}$$

There is no support for the second case. These conditions give the limits of integration in the case $q^2 \geq 0$ (timelike). Hence :

$$I(T) = \frac{2\pi}{2(2\pi)^4 2|\vec{q}|} \int_{\frac{\omega - |\vec{q}|}{2}}^{\frac{\omega + |\vec{q}|}{2}} d|\vec{k}| n_F(|\vec{k}|)$$

Changing the variable:

$$\begin{cases} |\vec{k}| = \frac{\omega + |\vec{q}|x}{2}; & d|\vec{k}| = \frac{|\vec{q}|}{2} dx \\ x = \frac{2|\vec{k}| - \omega}{|\vec{q}|} \end{cases}$$

$$I(T) = \frac{1}{(2\pi)^4} \frac{\pi}{4} \int_{-1}^1 dx n_F\left(\frac{\omega + |\vec{q}|x}{2}\right)$$

$$I(T) = \int \frac{d^4k}{(2\pi)^4} n_F(|k_o|) \delta(k^2) \delta^+((k-q)^2) = \frac{1}{(2\pi)^4} \frac{\pi}{4} \int_{-1}^1 dx n_F\left(\frac{|\vec{q}|x + \omega}{2}\right) \quad (\text{C.21})$$

Similarly one can prove that:

$$I'(T) = \int \frac{d^4k}{(2\pi)^4} n_F(|(k-q)_o|) \delta^+(k^2) \delta((k-q)^2) = \frac{1}{(2\pi)^4} \frac{\pi}{4} \int_{-1}^1 dx n_F\left(\frac{|\vec{q}|x - \omega}{2}\right) \quad (\text{C.22})$$

so that :

$$\text{Im } \Pi_5^{(+)}(q^2, T) = \frac{3}{8\pi} (m_u + m_d) \left\{ 1 - \frac{1}{2} \int_{-1}^1 dx \left[n_F\left(\frac{|\vec{q}|x + \omega}{2}\right) + n_F\left(\frac{|\vec{q}|x - \omega}{2}\right) \right] \right\} \quad (\text{C.23})$$

In the case $q^2 \leq 0$ (spacelike):

$$-1 \leq \frac{2\omega |\vec{k}| - (\omega + |\vec{q}|)(\omega - |\vec{q}|)}{2|\vec{k}||\vec{q}|} \leq 1$$

in the limit $|\vec{k}| \rightarrow \infty$

$$-1 \leq \frac{\omega}{|\vec{q}|} \leq 1$$

so that $|\vec{k}| \rightarrow \infty$ is part of the integration (the upper limit).

In the limit $\omega \rightarrow 0$

$$-1 \leq \frac{|\vec{q}|}{2|\vec{k}|} \leq 1$$

So that $|\vec{k}| \geq \frac{|\vec{q}|}{2}$ is the lowest limit. Both $\omega = -|\vec{q}|$ and $\omega = |\vec{q}|$ contribute to

the integral. For $\omega = 0$, $x = \frac{2|\vec{k}| - \omega}{|\vec{q}|} = 1$.

Using the fact that $1 = \frac{1}{2} \int_{-1}^1 dx$, $\int_{-1}^1 dx = \frac{3}{2} \int_{-1}^1 dx(1-x^2)$, and $\int_0^{|\vec{q}|^2} d\omega^2 \left(\frac{\omega}{|\vec{q}|^3}\right) = \frac{2}{3}$ $\left(\frac{\omega}{|\vec{q}|^3} \rightarrow \delta(\omega^2) \text{ when } |\vec{q}| \rightarrow 0\right)$,

$$\text{Im } \Pi_5^{(-)}(q^2, T) = \frac{\pi}{2} T^2 (m_u + m_d)^2 \delta(\omega^2) \quad (\text{C.24})$$

C.5 Some useful integrals

The following integrals [35] were also used during the calculations:

$$\int \frac{dx}{\sqrt{a+x^2}} = \ln(x + \sqrt{a+x^2}) \quad (\text{C.25})$$

$$\int \frac{dx}{(\sqrt{a+x^2})^3} = \frac{1}{a} \frac{x}{\sqrt{a+x^2}} \quad (\text{C.26})$$

$$\int_0^{s_o} \ln(2x + Q^2) dx = -\frac{Q^2}{2} \cdot \ln(Q^2) + \left[\frac{Q^2}{2} + s_o\right] \cdot \ln\left(\frac{Q^2}{2} + 2s_o\right) - s_o \quad (\text{C.27})$$

Appendix D

Some calculations

D.1 Some integral evaluations

Some more detailed steps made for the evaluation of 5.7 are the following:

$$\begin{aligned} \Pi_\mu(q) = & -4i \cdot N_c(m_u + m_d)^2 \int \frac{d^4k}{(2\pi)^4} \cdot \frac{1}{k^2(k-p)^2(k-p')^2} \cdot \\ & \left\{ (k-p')_\mu k \cdot (k-p) + (k-p)_\mu k \cdot (k-p') - k_\mu (k-p)(k-p') \right\} \end{aligned} \quad (\text{D.1})$$

or

$$\Pi_\mu(q) = -4i \cdot N_c(m_u + m_d)^2 \cdot \left\{ I_\mu - (p_\mu + p'_\mu)I + (p'_\mu p_\alpha + p'_\alpha p_\mu)I_\alpha - (pp')g_{\mu\alpha}I_\alpha \right\} \quad (\text{D.2})$$

where

$$I = \int \frac{d^4k}{(2\pi)^4} \frac{k^2}{k^2(k-p)^2(k-p')^2} \quad (\text{D.3})$$

$$I_\mu = \int \frac{d^4k}{(2\pi)^4} \frac{k_\mu k^2}{k^2(k-p)^2(k-p')^2} \quad (\text{D.4})$$

and

$$I_\alpha = \int \frac{d^4k}{(2\pi)^4} \frac{k_\alpha}{k^2(k-p)^2(k-p')^2} \quad (\text{D.5})$$

D.2. A FEW MORE DETAILED STEPS TO DETERMINE THE FINAL FORM OF $F(S, S', Q^2)$,

I_α being a function of $p_\mu + p'_\mu$, a part of $(p'_\mu p_\alpha + p'_\alpha p_\mu)I_\alpha$ will annihilate $(pp')g_{\mu\alpha}I_\alpha$ and the other does not have the desired form. $\Pi_\mu(q)$ becomes:

$$\Pi_\mu(q) = -12i(m_u + m_d)^2 \cdot \left\{ \int \frac{d^4k}{(2\pi)^4} \frac{k_\mu}{(k-p)^2(k-p')^2} - (p_\mu + p'_\mu) \int \frac{d^4k}{(2\pi)^4} \frac{1}{(k-p)^2(k-p')^2} \right\} \quad (\text{D.6})$$

Substituting $(k-p) \rightarrow k$ ($k-p' \rightarrow k-q$), and using the integrals evaluated in Appendix C.2, one gets:

$$\Pi_\mu(q) = \frac{3}{8\pi^2}(m_u + m_d)^2(p_\mu + p'_\mu) \ln\left(-\frac{q^2}{\nu^2}\right) \quad (\text{D.7})$$

D.2 A few more detailed steps to determine the final form of $F(s, s', Q^2, T)$

The part in $\text{Im } \Pi_1(s, s', Q^2, T)$ (see 5.35) that contains all the information referring to the thermal correction is $F(s, s', Q^2, T)$.

$$F(s, s', Q^2, T) = 1 - n_F(|k_o|) - n_F(|k_o - p_o|) - n_F(|k_o - p'_o|) + n_F(|k_o - p_o|) \cdot n_F(|k_o - p'_o|) + n_F(|k_o|) \cdot n_F(|k_o - p_o|) + n_F(|k_o|) \cdot n_F(|k_o - p'_o|) \quad (\text{D.8})$$

As in the zero temperature case, where integrals evaluated in [52] were used, to get 5.34, an integral of the following type was evaluated:

$$I = \int d^4k \delta(k^2) \cdot \delta((p-k)^2) \cdot \delta((p'-k)^2) \quad (\text{D.9})$$

For convenience, a frame where the three momentum of p^μ and p'^μ are parallel ($\vec{p} \parallel \vec{p}'$) can be chosen. Then:

$$\delta(k^2) = \frac{1}{2|\vec{k}|} \left\{ \delta(k_o - |\vec{k}|) + \delta(k_o + |\vec{k}|) \right\} \quad (\text{D.10})$$

$$\delta((p-k)^2) = \delta \left[p^2 - 2(k_o p_o - |\vec{k}| |\vec{p}| \cos \theta) \right] \quad (\text{D.11})$$

$$\delta((p'-k)^2) = \delta \left[p'^2 - 2(k_o p'_o - |\vec{k}| |\vec{p}'| \cos \theta) \right] \quad (\text{D.12})$$

D.2. A FEW MORE DETAILED STEPS TO DETERMINE THE FINAL FORM OF $F(S,$

where $p^\mu = (p_o, |\vec{p}|)$, $p'^\mu = (p'_o, |\vec{p}'|)$, $k = (k_o, |\vec{k}|)$ and θ is the angle between \vec{p} and \vec{k} .

From D.12,

$$\cos \theta = \frac{p'^2 - 2k_o p'_o}{2|\vec{k}||\vec{p}'|} \quad (\text{D.13})$$

and substituting D.13 into D.11,

$$k_o = \frac{1}{2} \frac{p^2 \frac{|\vec{p}'|}{|\vec{p}|} + |\vec{p}| p'^2}{p_o \frac{|\vec{p}'|}{|\vec{p}|} + |\vec{p}| p'_o} \quad (\text{D.14})$$

Choosing a particular reference frame where $p^\mu = (p_o, 0)$, $p'^\mu = (p'_o, |\vec{p}'|)$, i.e. a frame at rest with respect to the pion heat bath:

$$k_o = \frac{1}{2} p_o = \frac{1}{2} \sqrt{p^2} = \frac{1}{2} \sqrt{s} = \frac{1}{2} \sqrt{\frac{x+y}{2}} \quad (\text{D.15})$$

$$k_o - p_o = -\frac{1}{2} \sqrt{\frac{x+y}{2}} \quad (\text{D.16})$$

and

$$k_o - p'_o = -\frac{\frac{x-y}{2} + Q^2}{\sqrt{2(x+y)}} \quad (\text{D.17})$$

where the notation $p^2 = s$, $q = p' - p$, $Q^2 = -q^2$ was used. In this notation:

$$n_F(|k_o|) = n_1 = n_F\left(\left|\frac{1}{2}\sqrt{\frac{x+y}{2}}\right|\right) = n_F(|k_o - p_o|) = n_2 = n\left(\left|-\frac{1}{2}\sqrt{\frac{x+y}{2}}\right|\right)$$

and

$$n_F(|k_o - p'_o|) = n_3 = n_F\left(\left|\frac{Q^2 + \frac{x-y}{2}}{\sqrt{2(x+y)}}\right|\right)$$

so that D.8 becomes:

$$F(s, s', Q^2, T) = 1 - n_1 - n_2 - n_3 + n_1 n_2 + n_2 n_3 + n_1 n_3 \quad (\text{D.18})$$

D.2. A FEW MORE DETAILED STEPS TO DETERMINE THE FINAL FORM OF $F(S, S', Q^2, \dots)$

Bibliography

- [1] M. Abramowitz, I.A. Stegun, *Pocket book of Mathematical Functions*, (Verlag Harri Deutsch, Thun-Frankfurt/Main, 1984).
- [2] A. Barducci, R. Casalbuoni, S. de Curtis, R. Gatto, G. Pettini, *Phys.Lett. B* **244** (1990) 311.
- [3] A. Barducci, R. Casalbuoni, S. de Curtis, R. Gatto, G. Pettini, *Phys.Rev. D* **46** (1991) 2203.
- [4] C.J. Bebek et al., *Phys.Rev. D* **17** (1978) 1693.
- [5] Becchi et al., *Z.Phys. C* **9** (1981) 335.
- [6] M. Le Bellac, *Thermal Field Theory*, (Cambridge University Press, 1996).
- [7] M. Le Bellac, H.Mabilat, *Phys.Lett. B* **381** (1996) 262.
- [8] R.A. Bertlmann et al., *Z.Phys. C, Particles & Fields*, **39** (1988) 63.
- [9] A.I. Bochkarev, M.E. Shaposnikov, *Nucl.Phys. B* **268** (1985) 220.
- [10] A.I. Bochkarev, J Kapusta, *Phys.Rev. D* **54** (1996) 4066.
- [11] D.C. Cheng, G.K. O'Neill, *Elementary Particle Physics-An Introduction*, (Addison-Wesley 1979) p.92.
- [12] T.D. Cohen et al., University of Maryland PP#95-108, DOE/ER/40762-056.
- [13] C. Contreras, M. Loewe, *Int.J.Mod.Phys A* **5** (1990) 2297.

- [14] L. Dolan, R. Jackiw, Phys.Rev.D **9** (1974) 3320.
- [15] C.A. Dominguez, UCT report No UCT-TP-218/94 and hep-ph/9410363.
- [16] C.A. Dominguez, Phys.Rev. D **25** (1982) 3084; Mod. Phys. Lett. A **2** (1987) 983.
- [17] C.A. Dominguez, M.S. Fetea, M. Loewe, Phys.Lett. B **387** (1996) 151, Proc.Supp. Nucl.Phys. **54 A** (1997) 333.
- [18] C.A. Dominguez, M.S. Fetea, M. Loewe, Phys.Lett. B **406** (1997) 149, Proc.Supp. Nucl.Phys. (1997) .
- [19] C.A. Dominguez, M. Loewe, Phys.Rev. D **52** (1995) 3143.
- [20] C.A. Dominguez, E.de Rafael, Ann.Phys.(N.Y.) **174** (1987) 372.
- [21] C.A. Dominguez, M. Loewe, Phys.Lett. B **233** (1989) 201.
- [22] C.A. Dominguez, M. Loewe, Z.Phys. C, *Particles & Fields*, **49** (1991) 423.
- [23] C.A. Dominguez, M. Loewe, Z.Phys. C, *Particles & Fields*, **51** (1991) 69.
- [24] C.A. Dominguez, M. Loewe, J.C. Rojas, Z.Phys. C, *Particles & Fields*, **59** (1993) 63.
- [25] C.A. Dominguez, M. Loewe, J.S. Rozowsky, Phys.Lett. B **335** (1994) 506.
- [26] W.de Alfaro et al., *Currents in Hadron Physics* (North-Holland / American Elsevier 1973).
- [27] V.L. Eletsky, B.L. Ioffe, Phys.Rev.D **47**, (1993) 3083.
- [28] B.L. Ioffe, A.V. Smilga, Nucl.Phys. B **216** (1983) 373.
- [29] C Gale, J.I. Kapusta, Nucl.Phys. B **357** (1991) 65.
- [30] J. Gasser, H. Leutwyler, Phys.Lett. B **184** (1987) 83.

- [31] M.Gell-Mann, R.Oakes, B.Renner, *Phys.Rev.* **175** (1968) 2195.
- [32] P.Gerber, H.Leutwyler, *Nucl.Phys. B* **321** (1989) 387.
- [33] V. Giménez, J. Bordes, J. Peñarrocha, *Nucl.Phys. B* **357** (1991) 3.
- [34] M. Gourdin, *Proc. 6th Int. Symp. on Electron and Photon Interactions* (H. Rollnik and W. Pfeif, eds.), North-Holland, Amsterdam, p.412. 1973.
- [35] I.S. Gradshteyn, I.M. Ryzhik, *Table of Integrals, Series and Products* (New York Academic Press 5th Edition, 1980).
- [36] W. Greiner, A. Schäfer, *Quantum Chromodynamics* (Springer-Verlag 1995).
- [37] D. Griffiths, *Introduction to Elementary particles* (Harper&Row, NY, 1987).
- [38] B.L. Ioffe, A.V. Smilga, *Nucl.Phys. B* **216** (1983) 373.
- [39] L.D. Landau, *ZhETF* **37** (1958) 805.
- [40] A. Larsen, *Z.Phys. C, Particles & Fields*, **33** (1986) 291.
- [41] J. Kapusta, *Finite-temperature Field Theory*, (Cambridge University Press 1989)
- [42] K. Maltman, *Phys.Rev. D* **53** (1996) 2563.
- [43] M.V. Margvelashvili, M.E. Shaposhnikov, *Yad. Fiz* **47** (1988) 1752.
- [44] T. Muta, *Foundations of Quantum Chromodynamics*, (World Scientific, Singapore, 1987).
- [45] S. Narison, N. Paver, *Z.Phys. C, Particles & Fields*, **22** (1984) 69.
- [46] S. Narison, et all.,*Nucl.Phys. B* **212** (1983) 365.
- [47] N.F. Nasrallah, *Phys.Lett. B* **384** (1996) 263.
- [48] V.A. Nesterenko, A.V. Radyushkin. *Phys.Lett. B* **115** (1982) 410;
V.L. Eletsky, Ya. I. Kogan, *Z.Phys. C, Particles & Fields*, **20** (1983) 357;
K.G. Chetyrkin, A.B. Krasulin, V.A. Mateev, *JETP Lett.* **41** (1985) 272.

- [49] V.A. Novikov, M.A. Shifman, A.I. Vainshtein, V.I. Zakharov, Nucl.Phys. **B 249** (1985) 445.
- [50] Particle Data Group, R.M. Barnett et al, Phys.Rev. **D 54** (1996) 1.
- [51] P. Pascual, R. Tarrach, QCD: Renormalization for the Practitioner.(Springer-Verlag 1984).
- [52] H.Pietschmann, *Weak Interactions-Formulae, Results and Derivations*, (Springer-Verlag, 1983) 187.
- [53] P. Ramond, *Field Theory: A Modern Primer*, (Addison-Wesley 1994).
- [54] L.J. Reinders, H. Rubinstein,S. Yazaki., Phys.Rep. **127** (1985) 1.
- [55] W.B. Rolnick, *The Fundamental Particles and their Interactions* (Addison-Wesley 1994).
- [56] J.J. Sakurai, *Currents and Mesons*, (Univ. of Chicago Press 1969).
- [57] A.Schenk Nucl.Phys. **B 363** (1991) 97.
- [58] M.A. Shifman, A.I. Vainshtein, V.I. Zakharov, Nucl.Phys. **B 147** (1979) 385, 448, 519.
- [59] M.A. Shifman, *Vacuum Structure and QCD Sum Rules*, (North-Holland 1992).
- [60] E.V.Shuryak, *The QCD Vacuum, Hadrons and Superdense Matter*, (World Scientific, Singapore, 1988).
- [61] D.Toublan, Phys.Rev.**D 56**, (1997) 5629.
- [62] W.T. Vetterling et al., *Numerical Recipes-Example Book (Pascal)*, (Cambridge University Press 1986).
- [63] K.G. Wilson, Phys.Rev.**179** (1969) 1499.